

Hydrodynamic studies of 3D-Multiphase Flow of Gas-Liquid-Liquid Three-Phase Flow in a Pipe at Two Different Bend Angles and their Resultant Pressure Drops.



By

Muhammad Asif Siddique

(Registration No: 00000328543)

School of Chemical and Materials Engineering

National University of Sciences & Technology (NUST)

Islamabad, Pakistan

(2023)

Hydrodynamic studies of 3D-Multiphase Flow of Gas-Liquid-Liquid Three-Phase Flow in a Pipe at Two Different Bend Angles and their Resultant Pressure Drops.



By

Muhammad Asif Siddique

(Registration No: 00000328543)

A thesis submitted to the National University of Sciences and Technology, Islamabad,

in partial fulfillment of the requirements for the degree of

Master of Science in
Chemical Engineering

Supervisor: Dr. Umair Sikandar

Co-Supervisor: Dr. Muhammad Waqas Yaqub

School of Chemical and Materials Engineering

National University of Sciences & Technology (NUST)

Islamabad, Pakistan

(2023)



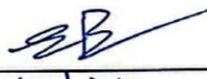
THESIS ACCEPTANCE CERTIFICATE

Certified that final copy of MS thesis written by Mr Muhammad Asif Siddique (Registration No 00000328543), of School of Chemical & Materials Engineering (SCME) has been vetted by undersigned, found complete in all respects as per NUST Statues/Regulations, is free of plagiarism, errors, and mistakes and is accepted as partial fulfillment for award of MS degree. It is further certified that necessary amendments as pointed out by GEC members of the scholar have also been incorporated in the said thesis.

Signature: 

Name of Supervisor: Dr Umair Sikandar

Date: 12 - 02 - 24

Signature (HOD): 

Date: 12/2/24

Signature (Dean/Principal): 

Date: 13 - 04 - 2024

① Plagiarism Report

② Thesis submission certificate by Library



Form III-1
(Must be type written)

National University of Sciences & Technology (NUST)
MASTER'S THESIS WORK
Formulation of Guidance and Examination Committee
(GEC)

Name: Muhammad Asif Siddique

NUST Reg. No: 00000328543

Department: Chemical Engineering (SCME)

Specialization: Chemical Engineering

Credit Hour Completed: 24

CGPA: 3.25

Course Work Completed

S/No	Code	Title	Core/Elective	CH	Grade
1	EME 921	Momentum Heat and Mass Transfer	Core	03	B
2	CHE 843	Separation Processes in Chemical Engineering	Core	03	B+
3	CHE 853	Green Process Engineering	Elective	03	B
4	RM 898	Research Methodology	Elective	02	Q
5	CHE-847	Chemical Kinetics & reactor design	Core	03	B
6	EME-981	Industrial Catalysis for Energy Systems	Elective	03	A
7	CHE-814	Product Technology	Elective	03	B+
8	CHE 848	Gasification processes	Elective	03	B
9	ESE 911	Carbon Capture and Utilization	Elective	03	B

Date: 03-03-2022

Student's Signature: [Signature]

Thesis Committee

1. Name: Dr. Umair Sikandar (Supervisor)
Department: SCME

Signature: [Signature]

2. Name: Dr. Muhammad Waqas Yaqub (Co-Supervisor)
Department: Deputy Director Research (Projects)

Signature: [Signature]

3. Name: Dr. Muhammad Ahsan (GEC)
Department: SCME

Signature: [Signature]

4. Name: Dr. Muhammad Nouman Aslam Khan (GEC)
Department: SCME

Signature: [Signature]

Date: 29/3/22

Signature of Head of Department: [Signature]

Date: 29.3.2022

APPROVAL
Signature of Dean/Principal: [Signature]

Distribution

1x copy to Exam Branch, Main Office NUST

1x copy to PGP Dte, Main Office NUST

1x copy to Exam branch, respective institute

School of Chemical and Materials Engineering (SCME) Sector H-12, Islamabad



Form: TH-04

National University of Sciences & Technology (NUST)

MASTER'S THESIS WORK

We hereby recommend that the dissertation prepared under our supervision by

Regn No & Name: 00000328543 Muhammad Asif Siddique


Title: Hydrodynamic Studies of the 3D-Multiphase Flow of Gas-Liquid-Liquid Three-Phase Flow in a Pipe at Two Different Bend Angles and their Resultant Pressure Drop.

Presented on: 14 Dec 2023 at: 1400 hrs in SCME (Conference Room)

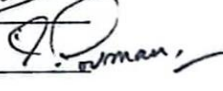
Be accepted in partial fulfillment of the requirements for the award of Master of Science degree in Chemical Engineering.

Guidance & Examination Committee Members

Name: Dr Muhammad Ahsan (GEC)

Signature: 

Name: Dr Muhammad Nouman Aslam Khan (GEC)

Signature: 


Name: Dr Muhammad Waqas Yaqub (Co-Supervisor)

Signature: 

Supervisor's Name: Dr Umair Sikandar

Signature: 

Dated: 17-1-24


Head of Department

Date 29/1/24


Dean/Principal

Date 17-1-24

2.2.2024

School of Chemical & Materials Engineering (SCME)

AUTHOR'S DECLARATION

I Muhammad Asif Siddique hereby state that my MS thesis titled “ Hydrodynamic Studies of 3D-Multiphase Flow of Gas-Liquid-Liquid Three-Phase Flow in a Pipe at Two Different Bend Angles and Their Resultant Pressure Drops is my own work and has not been submitted previously by me for taking any degree from the National University of Sciences and Technology, Islamabad, or anywhere else in the country/world.

At any time, if my statement is found to be incorrect even after I graduate, the university has the right to withdraw my MS degree.

Name: Muhammad Asif Siddique

Date: 14-12-2023

PLAGIARISM UNDERTAKING

I solemnly declare that the research work presented in the thesis titled “ Hydrodynamic Studies of 3D-Multiphase Flow of Gas-Liquid-Liquid Three-Phase Flow in a Pipe at Two Different Bend Angles and Their Resultant Pressure Drops. ” is solely my research work with no significant contribution from any other person. Small contribution/ help wherever taken has been duly acknowledged and that complete thesis has been written by me.

I understand the zero-tolerance policy of the HEC and the National University of Sciences and Technology (NUST), Islamabad towards plagiarism. Therefore, I as an author of the above-titled thesis declare that no portion of my thesis has been plagiarized and any material used as reference is properly referred to/cited.

I undertake that if I am found guilty of any formal plagiarism in the above-titled thesis even after the award of my MS degree, the University reserves the right to withdraw/revoke my MS degree and that HEC and NUST, Islamabad has the right to publish my name on the HEC/University website on which names of students are placed who submitted plagiarized thesis.

Signature



Name: Muhammad Asif Siddique

Date: 14-12-2023

DEDICATION

By the grace of **Almighty Allah**, who is the most Compassionate and Merciful.

This study is sincerely dedicated to my beloved **Parents** and my **Family**, especially my brother **Nasir Aziz** and **my Wife**, who has always been my source of guidance and support.

To my **supervisor** who shared his knowledge, gave advice, and encouraged me to fulfill my objectives.

And to all my fellows I worked with and enjoyed wonderful memories.

ACKNOWLEDGMENTS

All praises to **Almighty Allah**, whose unwavering blessings and guidance have illuminated my path and fueled my determination, who blessed us with the ability to think and made us willing to explore the universe. Infinite greetings to the **Holy Prophet Muhammad (PBUH)**, the cause of the universe's creation and a fountain of knowledge and blessing for all humanity.

I wish to convey my sincere gratitude to my supervisor, **Dr. Umair Sikandar**, for his exceptional mentorship, firm support, and profound insights. Your expertise and dedication have been pivotal in determining my research and developing my growth as a scholar. I am incredibly lucky to have had the privilege to learn from you. I am equally indebted to my co-supervisor, and my sincere gratitude to **Dr. Muhammad Waqas Yaqub** for his invaluable guidance, which has been instrumental in refining and broadening my perspectives. I also extend heartfelt appreciation to the esteemed members of the GEC, **Dr. Muhammad Ahsan**, and **Dr. Muhammad Nouman Aslam Khan**, whose valuable feedback and commitment to academic excellence have significantly promoted the value of my research.

My gratitude extends to my beloved **Parents**, whose unconditional love, support, and sacrifices were the cornerstone of my destination. Your trust in me has proved to be a valuable pillar for my continuous success, and I'm humbled by your constant support.

To my brother **Nasir Aziz** and **my Dearest Wife**, your unwavering patience, understanding, and encouragement have been my anchor during this challenging endeavor. Your belief in my abilities has propelled me forward, and I am obliged for your steady encouragement and everything you have done for me.

I am modestly thankful for the support and assistance from lab staff at SCME and at SINES, whose dedication has ensured a conducive research environment. My heartfelt thanks to my fellow lab mates and colleagues who have shared their knowledge on this journey. Your exchange of ideas and collaborative spirit have enriched my experience and made this journey memorable.

Muhammad Asif Siddique

TABLE OF CONTENTS

ACKNOWLEDGMENTS.....	ix
TABLE OF CONTENTS.....	xi
LIST OF TABLES	xiii
LIST OF FIGURES	xiv
LIST OF SYMBOLS, ABBREVIATIONS, AND ACRONYMS	xvi
ABSTRACT	xvii
1 CHAPTER 1 INTRODUCTION.....	1
1.1. Background	1
1.2. Flow Patterns of Three-Phase Flow in Pipelines.....	2
1.2.1. Horizontal Three-Phase Flow.....	4
1.2.1.1. Pressure Drops During the Horizontal Three-Phase Flow.....	4
1.2.2. Three-Phase Flow in Vertical Direction	5
1.2.2.1. Pressure Drops During the Vertical Three-Phase Flow.....	5
1.3. Computational Fluid Dynamics (CFD).....	6
1.4. Pressure Drops During the Flow Through the Bends	7
1.5. Problem Statement.....	7
1.6. Research Objectives.....	9
1.7. Scope of Study.....	9
2 CHAPTER 2 LITERATURE REVIEW.....	11
2.1. Background	11
2.2. Flow Patterns	12
2.3. Types of Flow Patterns	13
2.3.1. Horizontal Three-Phase Flow Patterns	13
2.3.1.1. Bubbly Flow	13
2.3.1.2. Stratified and Stratified Wavy Flow	14
2.3.1.3. Plug Flow	15
2.3.1.4. Slug Flow	16
2.3.1.5. Annular Flow.....	17
2.3.2. Flow Patterns of Three-Phase Flow in Vertical Orientation	18
2.3.2.1. Bubbly Flow	18
2.3.2.2. Slug Flow	19
2.3.2.3. Plug Flow	20

2.3.2.4.	Churn Flow	21
2.3.2.5.	Annular Flow	22
2.4.	Multiphase Flows.....	25
2.4.1.	Two-Phase Flow	25
2.4.1.1.	Experimental Literature on Two-Phase Flows	25
2.4.1.2.	Modeling Literature on Two-Phase Flows.....	26
2.4.2.	Three-Phase Flow	27
2.4.2.1.	Experimental Literature on Three-Phase Flows	27
2.4.2.2.	Modeling Literature on Three-Phase Flows.....	28
2.5.	Pressure Drop Prediction Models	28
3	CHAPTER 3 METHODOLOGY	29
3.1	Geometry.....	29
3.2	Meshing.....	30
3.3	Multiphase Model.....	33
3.4	Governing Equations	34
3.5	Model of Turbulence Flow.....	35
3.6	Physical Properties and Boundary Conditions of the Fluids	35
3.7	The Time Step and Solver.....	36
4	CHAPTER 4 RESULTS AND DISCUSSIONS	38
4.1	CFD Simulations Results of Flow Patterns in the Bends	38
4.1.1	Three-Phase Flow Patterns in the 90° Bend.....	38
4.1.2	Three-Phase Flow Patterns in the 180° Bend	41
4.2	Pressure Drop Variations in the 90° Bend	43
4.3	Pressure Drop Variations in the 180° Bend	49
5	CHAPTER 5 CONCLUSION AND FUTURE RECOMMENDATIONS	53
6	REFERENCES	56

LIST OF TABLES

Table 1.1: Types of flow patterns [33]	5
Table 3.1: Mesh Quality Indicators.....	33
Table 3.2: Fluid's physical characteristics [5].....	36
Table 3.3: Boundary Conditions	36

LIST OF FIGURES

Figure 1.1: Types of Bend Angles.	1
Figure 2.1: Pipeline with different types of Bends	11
Figure 2.2: Three-phase bubbly Gas-Liquid-Liquid flow patterns [47]	13
Figure 2.3: Stratified three-phase flow patterns of Gas-Liquid-Liquid [47].....	14
Figure 2.4: Plug three-phase flow patterns of Gas-Liquid-Liquid [47].....	15
Figure 2.5: Slug three-phase flow patterns of Gas-Liquid-Liquid [47].....	16
Figure 2.6: Annular three-phase flow patterns of Gas-Liquid-Liquid [47].....	17
Figure 2.7: Vertical bubbly three-phase flow patterns of Gas-Oil-Water [47]	19
Figure 2.8: Vertical Slug three-phase flow patterns of Gas-Oil-Water [47].....	20
Figure 2.9: Vertical Plug three-phase flow patterns of Gas-Oil-Water [47]	21
Figure 2.10: Vertical Churn three-phase flow patterns of Gas-Oil-Water [47]	22
Figure 2.11: Vertical core-annular three-phase flow patterns of Gas-Oil-Water [47].....	23
Figure 2.12: Vertical core-annular three-phase flow patterns of Gas-Oil-Water [47].....	24
Figure 3.1: 90° bend geometry [5].....	29
Figure 3.2: 180° bend geometry.	30
Figure 3.3: Meshed geometry of 90° bend pipe.....	30
Figure 3.4: Meshed geometry of 180° bend pipe.	31
Figure 3.5: Mesh geometry of enlarged straight pipe section.	31
Figure 3.6: Meshed geometry of 90° bend section.	31
Figure 3.7: Meshed geometry of 180° bend section.	31
Figure 3.8: Mesh Independence analysis of 90° bend geometry.....	32
Figure 3.9: Mesh Independence analysis of 180° bend geometry.	32
Figure 4.1: Validations of simulation results of three-phase flow patterns in a 90° bend [5].....	40
Figure 4.2: Simulation results of three-phase flow patterns in a 180° bend.	42
Figure 4.3: Variation in pressure reduction in the 90° bend at a constant f_0 value of 0.5 and when the gas and liquid phases' surface velocities increase [5].....	43
Figure 4.4: Comparison of the CFD results at the 90° bend at a constant f_0 value of 0.5 and rising gas and liquid superficial velocities with the experimental findings for pressure drop.....	44
Figure 4.5: Variation in the 90° bend pressure drop with increasing gas and continuous liquid phase superficial velocities while maintaining a constant liquid surface velocity of 0.32 ms ⁻¹ [5].	45
Figure 4.6: Comparison of CFD and experimental pressure drop results in the 90° bend with a constant value of the liquid superficial velocity of 0.32 ms ⁻¹ with an increasing gas velocity and continuous liquid phase velocity.....	46
Figure 4.7: Pressure drop disparity in the 90° bend with rising gas and f_0 value and a constant liquid superficial velocity of 0.4 ms ⁻¹ [5].....	47
Figure 4.8: Comparison of CFD pressure drop results with experimental results in the 90° bend of a constant superficial velocity of liquid at 0.4 ms ⁻¹ with an increasing gas velocity and f_0 value. .	48
Figure 4.9: Variation in pressure drop in the 180° bend at a constant f_0 value of 0.5 with increasing gas and liquid phase superficial velocities.	50
Figure 4.10: Changes of pressure drop within 180° bend at a constant value of liquid superficial velocity of 0.32 ms ⁻¹ with an increasing gas phase superficial velocity and continuous liquid phase.	51

Figure 4.11: Variations in the 180° bend pressure drop at a constant liquid superficial velocity of 0.4 ms⁻¹ with an increasing gas phase superficial velocity and f_o value. 52

LIST OF SYMBOLS, ABBREVIATIONS, AND ACRONYMS

CFD	Computational Fluid Dynamics
VOF	Volume of Fluid
f_o	Oil-to-Liquid volume ratio
ObUL-WLB	Oil-based Upper Layer-Water Layer at the Bottom
WbUL-WLB	Water-based Upper Layer-Water Layer at the Bottom
SOW-MiF	Separate Oil and Water-Mixture at the Interface
SOW	Separate Oil and Water
ObM/WbM	Oil-based Mixture/Water-based Mixture
CAF	Core-Annular Flow
3D	Three-Dimensional
ID	Internal Diameter of the pipe
L/D ratio	Length to Diameter ratio
R/d ratio	Radius to diameter ratio

ABSTRACT

The phenomenon of flow of different phases flowing simultaneously in the pipelines of Petrochemical industries is of great interest. Different types of fittings and bends are used to connect these pipelines for transporting the fluids. The phenomenon becomes more complicated when more than two phases are flowing through it. Various flow patterns arise in the pipelines depending upon the individual superficial velocities of the phases and the type of bend. The radius to diameter (R/d) ratio, internal pipe's diameter, flow orientation, and inclination of the pipe have significant impacts on flow behavior. Bend offers restrictions which results in loss of pressure. The restriction, hydrostatic, and frictional losses lead to combined pressure losses within pipelines. The Computational Fluid Dynamics (CFD) software is a highly demanding tool that proves to be very impressive in examining fluid behavior, its characteristics, and fluid pressure drops. Simulating the multiphase flows can save the material setup experimental cost and human time to conduct the long hours of experiments. This study emphasizes the use of CFD software to analyze the pressure drop and flow patterns within the 90° and 180° bend pipes and compares them with the experimental work. The three-dimensional (3D) geometries of 90° and 180° bend pipes having 6 inches internal diameter and R/d ratio of 1 are used. Superficial velocities of the liquid, oil, and gas were in the limit of 0.08-0.36, 0.08-0.36, and 0.5-4 ms⁻¹ respectively. The CFD simulation results from pressure drops of a 90° bend pipe with a steady 0.5 oil-to-liquid volume ratio (f_o) value and increasing gas and oil velocities, at two f_o values of 0.25 and 0.75, and maintaining a steady 0.32 ms⁻¹ liquid velocity with increasing gas velocities, and at increasing f_o values from 0.2-0.8, maintaining at 0.4 ms⁻¹ liquid velocities with increasing gas velocities are compared with experimental work and have a maximum percentage error of 10.37%, 12.63%, and 9.03% respectively. Rolling wave pseudo-slug and slug flow patterns are three-phase flow patterns that were found at the 90° bend; these flow patterns were compared to experimental studies and demonstrated strong agreement. The pressure drops and the same flow patterns of the three-phase flow system were also analyzed in the 180° bend pipe.

Keywords: CFD; ANSYS Fluent; Simulations; Three-Phase Flow; Flow Patterns; Pressure Drop

CHAPTER 1 INTRODUCTION

1.1. Background

The phenomenon of flow of different phases flowing simultaneously is of great interest in the pipelines of many petrochemical and nuclear power generation industries [1]. The pipelines are used either to transport the fluids within the industries or to transport the fluids that are produced from the petroleum reservoirs. For the arrangement of the pipelines and their design, a comprehensive study and evaluation of the fluid dynamics in the pipes is very necessary [2]. These fluids flow in different phases. Single-phase, two-phase, or multiphase flows are mostly observed during fluid flow within industries such as chemical, gas oil, and many other industries [3]. The flow of single-phase is common but the study of more than one phase is complex, and their complexity increases more when a third one is added to them. Different flow patterns arise due to the two immiscible liquids, which differentiate the types of flows [4]. When flowing or transporting the fluids through pipelines, fittings, and bends are used to connect these pipes. The ratio of the bend's radius to its diameter (R/d), the pipe's internal diameter, orientation of flow, and pipe inclination attributes for the flow behavior [5-7]. Bend angles can be of different types like 45° , 90° , 135° , or 180° bend angles as shown in Figure 1.1.

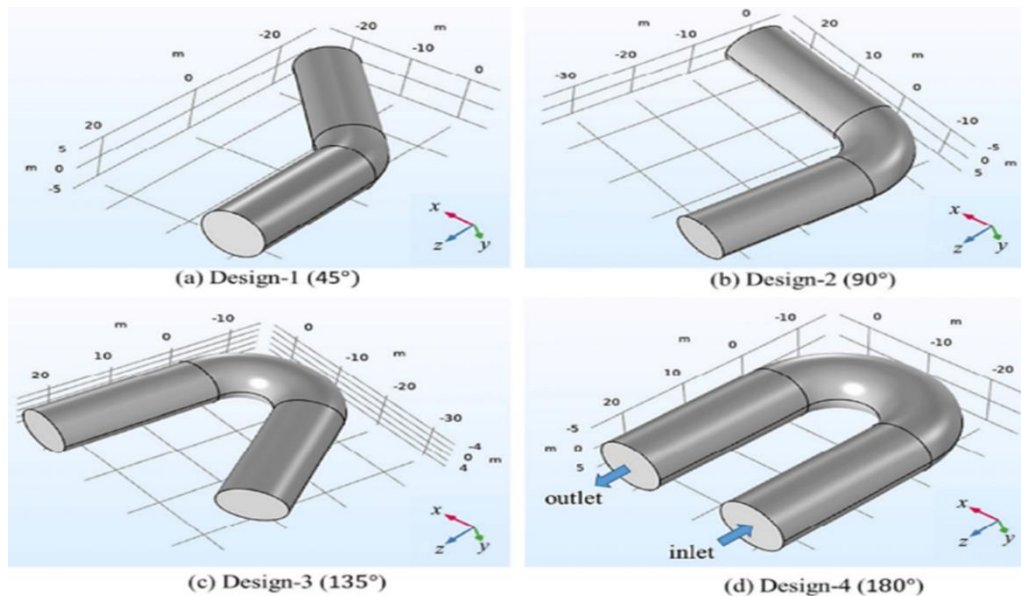


Figure 1.1: Types of Bend Angles.

When fluid passes through the bend, it is influenced by different kinds of forces which are gravitational and centrifugal [8]. Bend angle or curvature can increase the level of centrifugal forces because the decrease in the ratio of radius to diameter can sharpen the angle curvature. Therefore, the lower the ratio, the greater will be the induction of centrifugal force. The circular motion of the fluid is created because of the angle curvature. The liquid phase changes its velocity profile because the secondary flow is produced at the outer part of the curvature [9-11]. The boundary layer effect and centrifugal force both combined to produce this secondary flow [12]. These all change the patterns of flows and pressure drops within the pipelines having unlike bends. Turbulence is another factor that contributes to flow patterns, and the pressure drops because the turbulence can be increased due to the creation of the centrifugal and gravitational forces which leads to the kinetic energy dissipation. Therefore, pressure drops increase. [13-15]

Secondary flow in horizontal pipelines can only be obtained by anisotropy and non-homogeneity of the turbulence but they are very weak in strength. But in pipes having bends, secondary flow is induced by the combination of centrifugal forces and pressure gradient, and they can also affect the motion of the primary flows in the pipes which makes the flow characteristics very complicated in the pipe having bends [16]. When more phases are added to the flow, then fluid behavior becomes more complicated [17, 18]. Therefore, the various flow patterns are adopted because of the immediate flow of different phases. Those obtained flow patterns rely on the fluid's physical characteristics, the internal diameter of the pipe, and their flow rate [18, 19].

1.2. Flow Patterns of Three-Phase Flow in Pipelines

There are two primary categorizations of flow patterns of 3-phases: liquid-liquid and gas-liquid. When multiple phases flow concurrently within a closed conduit, an interfacial structure known as a flow pattern emerges. The predominant factors characterizing 3-phase flow patterns were the relationships in-between oil and water, as well as gas-liquid flow patterns. Water and oil can either flow as a combined mixture or in separate layers. In the case of mixed flow, one of these substances serves as the continuous phase, while the other assumes the role of the distributed phase [20]. The nature of the mixture fluid, whether it is water-based or oil-based, depends on the proportion of each liquid phase within the total mixture. In oil-based flow, various droplet sizes of water are separated within the continuous phase of oil, whereas in water-based flow, this arrangement is reversed. A transformation

from a water-based to an oil-based mixture occurs when the oil fraction within the total liquid increases during the mixing process in a water-based flow. This entire process of transitioning the constant liquid phase is named phase inversion. Notably, that phase inversion process typically leads to alterations within the characteristics of 3-phase flow.

The development of flow patterns is primarily influenced by several key parameters, namely superficial velocities, pipe inclination, physical properties of the fluids, and the internal diameter of the pipe involved. When maintaining a constant pipe internal diameter and phase properties, alterations in individual velocities of liquid and gas phases lead to shifts towards oil-water and liquid-gas flow patterns. Consequently, it is fundamental to gather information about the flow patterns that emerge at varying individual liquid and gas velocities.

Moreover, internal pipe diameter plays a substantial role in establishing the specific three-phase flow patterns under given conditions. When fluid flow rates remain constant, increasing the pipe's internal diameter results in reduced fluid velocity, which, in turn, minimizes pressure drop [21]. Additionally, the greater cross-sectional area of pipelines provides the liquids with more space to stay according to their densities.

The velocity of the mixture, oil-to-liquid volume ratio (f_o), and each phase's fraction are calculated by the following equations:

$$U_{mixture} = U_{gas} + U_{oil} + U_{water} \quad (1.1)$$

$$a_{gas} = \frac{U_{gas}}{U_{mixture}} \quad (1.2)$$

$$a_{oil} = \frac{U_{oil}}{U_{mixture}} \quad (1.3)$$

$$a_{water} = \frac{U_{water}}{U_{mixture}} \quad (1.4)$$

$$f_o = \frac{a_{oil}}{a_{oil} + a_{water}} \quad (1.5)$$

Three-phase flow patterns can be classified into horizontal straight and vertical flow patterns, based on the orientation of the flow.

1.2.1. Horizontal Three-Phase Flow

The most general gas-liquid straight flow patterns are annular, stratified, slug, plug, and bubbly flows [22-27]. Water and oil can either stream as a blend or in separate layers. In the case of mixed flow, one acts as the continuous phase, while the other serves as the distributed phase [20]. In scenarios where gas, oil, and water flow separately, their positions are determined by their respective densities. During stratified flow, the gas phase, being the lightest, typically occupies the uppermost layer, whereas the oil phase moves in the center of the pipeline due to its density being lower than water but higher than the gaseous phase. The phase of water, being the heaviest one, flows at the bottom because of its greater density compared to the other two phases. Plug and slug flow fall within the category of intermittent flows, where the liquid and gas phases move through the pipelines intermittently. In plug flow, gas, and liquid alternate in the shape of distinct plugs. Liquid surrounds gas bubbles, primarily flowing in the upper section of the pipelines [22]. During flows of slug, the coalescence of tiny gas foams results in the formation of larger gas bubbles known as Taylor bubbles. Bubbly flows occur when little gas bubbles disperse surrounded by the liquid phase. In annular flows, the liquid phase occupies both the upper and bottom sections of the pipeline, whereas the gas phase flows in the mid-section.

1.2.1.1. Pressure Drops During the Horizontal Three-Phase Flow

In a straight 3-phase flow system, the loss in pressure experiences variation according to the established flow patterns. Specifically, in the straight flow section, frictional loss is the dominant factor contributing to pressure drop [28]. When the pipeline maintains a constant inclination angle, static pressure losses are minimal, and momentum losses are negligible due to the consistent internal diameter of the pipe along its length. Consequently, the primary cause of pressure loss in horizontal 3-phase flow is the friction between the pipe and fluid.

Pressure losses are notably heightened when water and oil flow together in the form of a fluid blend, particularly in oil-based flows. This rise is recognized for the greater oil viscosity compared to the water phase, resulting in higher friction levels in oil-based flow. The elevated viscosity of the fluid mixture diminishes the flow capacity of the mixture, which in turn amplifies the pressure loss. This is because of the effective rise in viscosity as a result of water precipitations being dispersed within the phase of oil.

1.2.2. Three-Phase Flow in Vertical Direction

Vertical pipelines exhibit various three-phase flow patterns, with gravitational forces exerting a substantial influence. Consequently, when comparing similar superficial phase velocities, the flow structures in vertical and straight orientations diverge due to gravitational effects. In vertical orientation, the prevalent gas-liquid flow patterns comprise annular, churn, slug, and plug flow patterns [29-32]. During vertical direction, plug and slug patterns differ from their horizontal counterparts. This distinction arises from the presence of Taylor bubbles and gas plug flows in the middle of the pipe, with the liquid phase moving alongside the pipeline walls. The churn flow patterns are unique to vertical orientation. During churn flow, the gas phase typically elevates the liquid phase, but gravitational forces cause it to descend, resulting in an oscillatory flow. This generates a high degree of turbulence, leading to significant mixing of water and oil phases. Consequently, these two flows intermittently as a combined fluid. During annular flow in vertical pipelines, a liquid layer encases the gas core. This liquid layer can either move as an independent oil-water film or else as a liquid blend, depending on the degree of mixing induced by the phase's velocities.

1.2.2.1. Pressure Drops During the Vertical Three-Phase Flow

In vertical 3-phase flow, it is noticeable that pressure losses are more pronounced in comparison to horizontal three-phase flow. This disparity arises from the change in flow direction, transitioning from a horizontal to a vertical orientation. The frictional losses are not only the reason for pressure drop during the vertical orientation but because of the gravitational effect acting upon the fluid flowing upward direction, the hydrostatic losses also become more significant [28]. When oil, water, and gas exhibit low superficial velocities, gravitational forces become the prevailing influence. The dependency of the pressure drop on the frictional losses increases when the hydrostatic losses become less important with the escalation in flow velocity.

Table 1.1 presents the observed horizontal and vertical flow patterns [33].

Table 1.1: Types of flow patterns [33]

Sr. No.	Horizontal Flow	Vertical Flows
i.	Bubbly flow	Bubbly
ii.	Annular	Slug

iii.	Slug	Plug
iv.	Stratified wavy	Churn
v.	Stratified	Annular

These all patterns get more complicated during the three-phase flows moving in a pipe at different bend angles. Therefore, the relative position of each phase and local phase velocities are affected by the presence of the bend [11, 34]. The centrifugal forces induce the separation that leads to the increase of slip between the fluids [35, 36].

Due to the additional liquid phase, the immediate flow of liquid, gas, and oil becomes complicated by the presence of different kinds of bend angles. When all phases flow through the curvature of bends, the flow patterns are completely transformed, and a complicated flow structure is established when crossing the angle of the curvature because of the gravitational and centrifugal effects. Due to various flow patterns at different bend angles and flow rates, a three-phase flow system offers many problems such as pressure drops, liquid holdup, corrosion, and erosion [37, 38].

1.3. Computational Fluid Dynamics (CFD)

The Commercial CFD Software is a high-demand impressive tool to examine the fluid flow processes and their characteristics. It predicts the fluid flow behavior by using different computational methods which involve the solving of different kinds of complex and challenging governing equations like Navier-Stokes equations. This tool proves to have an impressive role in examining the fluid flow behavior, optimizations, and designing many different systems. By using iterative techniques and discretizing the fluid domain into many computational cells, CFD can help individuals acquire insights into turbulence features, pressure and velocity distributions, and flow patterns.

The CFD approach can also be suitable for analyzing different kinds of situations that are not feasible with laboratory experiments. By combining numerical methods, computational power, and advanced algorithms, CFD provides a versatile and powerful approach to studying fluid flow in pipelines. It complements experimental investigations and expands the understanding of complex flow phenomena, offering insights that are often not feasible or practical to obtain through laboratory experiments alone [32].

The multiphase model of Volume of fluid (VOF) is among the models applied during simulation which tracks fluid volume within the complete domain of the fluid. It is a widely used technique in CFD for simulating multiphase flows which enables the accurate and precise prediction of the phase interaction and volume of fluid. The volume fraction characterizes each cell of the fluid domain which represents that each cell of the fluid domain is occupied by the proportion of the fluid. The discretization of the volume fraction is computed by the VOF model as the fluid moves forward in the cells and interacts which allows to simulate the phenomena like gas-liquid interfaces.

1.4. Pressure Drops During the Flow Through the Bends

There are various factors based on geometry such as flow patterns, superficial phase flow rates, fluid categories used, and many other factors on which the pressure reduction depends during flow through the bends. The frictional, restriction, and hydrostatic losses result in a combined pressure drop during the vertical bend which indicates that the capacity of the flow can be reduced significantly due to the pressure losses during the flow through the bends [39].

The maintenance cost of the equipment increases, and the effective life of the flow systems decreases because the liquid phase continuously wets the walls of the pipelines which results in corrosion and erosion in the downstream pipe's walls and the outer curvature wall. The liquid holdup within the upstream pipe increases because the curvature of the bend offers some restrictions which results in a rise in the liquid phase level in the pipelines having vertical bend. The centrifugal forces are induced in the fluid flow because of pipe curvature [40]. Due to disparities in density between the gas phase and fluid, centrifugal forces lead to the gas phase flowing along the pipe's inner wall and the liquid along the pipe's outer curvature wall. As flow ascends in the upright portion of the bend, flow experiences a gravitational pull due to the force of gravity. The flow becomes more turbulent as compared to the straight pipe because of the impacts of both forces. The direction of the flow changes when the fluid moves through the bend from a horizontal straight section to a vertical orientation. Therefore, at the same superficial velocities, the flow type could be of different types in both sections.

1.5. Problem Statement

The pipelines are commonly used equipment to transport the produced fluid mixture of water, oil, and gas from the onshore and seaward reservoirs to the target oil and gas processing facilities. During the

transportation of these mixtures of three-phase flows in the pipeline, networks encounter different kinds of problems such as loss in pressure. Therefore, the pressure losses lead to substantial electricity costs as pumps and turbines are used to flow the fluids. Hence, for designing and operating the multiphase flow system effectively and efficiently, the role of fluid flow behavior and its characteristics is very necessary.

The concurrent flow of gas and two non-miscible liquids exhibits various flow patterns at distinct individual fluid flow rates which are associated with the governing conditions. The predominant 3-phase flow patterns primarily hinge on considerations like the pipe's geometry, physical characteristics of the liquids involved, the pipe's inclination, and the velocities of the fluids. The horizontal and vertical pipelines could have different kinds of flow patterns at the same boundary conditions and parameters. To redirect the flow in various directions, horizontal and vertical pipelines are typically connected using various types of bend angles. The complexity of the flow increases as it passes through the curves because flow encounters produce centrifugal and gravitational forces in the bend. Mostly a 90° bend is utilized to link the horizontal and vertical pipelines. The bend just doesn't influence the flow, but flow patterns and their characteristics are also substantially changed by the occurrence of the curvature. This results in a major loss of pressure in the pipelines.

The past survey of literature claimed that the drop in the pressure of simultaneously flowing liquid, oil, and gas 3-phase flow is limited to straight horizontal pipelines and only to upstream of 90° bend experimentally. Therefore, there have been no studies conducted to numerically investigate the pressure loss in a 3-phase flow within a pipeline at various bend angles. Hence, there is a need to conduct a numerical setup to predict the variation of liquid-oil-gas pressure losses in a pipe with different bend angles by adopting the CFD software tool.

The current numerical configuration has been established to analyze flow patterns of 3-phase systems and their resultant pressure drop involving water, oil, and gas in the 90° bend and 180° bend angles having a diameter of 6 inches using the commercial CFD ANSYS Fluent. The research findings would give important perceptions of 3-phase flow dynamics and the consequent pressure drop comparisons between 90° bend and 180° bend, which would prove beneficial in designing, optimizing, and enhancing the efficiency of 3-phase flow systems.

1.6. Research Objectives

The present study is majorly concerned with the physical characteristics and drop in pressure of the fluids within the pipelines at different bend angles and flow rates using Computational Fluid Dynamics (CFD). The pressure loss is remarkably affected because of high degree turbulence and complex flow patterns developed while flowing within the pipe having bends. The bend offers restriction and frictional losses which collectively result in pressure drop across the bend [41, 42]. Early research on examining and forecasting the pressure drops in the multi-phase flows has been reported but limited to the horizontal flows and only limited to a 90° bend angle [43, 44].

The physical characteristics and loss in pressure of multi-phase flows within the pipe at different bend angles is a major concern shown by the present literature survey. Therefore, investigations through commercial Computational Fluid Dynamics (CFD) are more reliable and efficient. The experimental information published in the past literature can validate these investigations.

The objective of the proposed topic is as follows:

- Comparison of fluid properties when flowing in a straight pipe and a pipe of different bend-angles
- Overall behavior of three-phase flow through CFD Analysis.
- To improve the efficiency of the Flow System.
- Comparison of CFD simulation results with the previous experimental results.

To reduce the cost associated with obtaining the material to establish the experimental setup and to reduce the human work hours for experimenting, the CFD tool is proposed as the best reliable alternative [45]. CFD program can provide accurate results with minimum errors, and it has the potential to replicate the findings of the experiment model with a minimum percentage error value of less than 5% [46].

1.7. Scope of Study

The CFD investigation of the 3-phase flow was carried out using Ansys Fluent. The geometry of two pipes 90° and 180° bend was constructed in SolidWorks software. The dimensions of the constructed pipes were based on the physical pipe used in the experimental work. To simulate the 3-phase flow, the VOF and turbulence models were used in the multiphase model. Different flow patterns and their resultant pressure drops across the 90° and 180° bend pipes were analyzed. The pressure drops and

flow patterns results obtained from CFD simulations were compared with the experimental work and showed strong agreement.

Different pipe bends are used in the multiphase flow system which could result in loss of pressure. This pressure loss led to substantial electricity costs because pumps and turbines were used to flow the fluids. Various flow patterns arise during the flow through the bends which also increases the pressure losses.

- Use of CFD tool to examine the 3-phase flow patterns and to improve the efficiency of the flow system.
- Pressure drop prediction through the CFD tool to minimize the electricity cost.
- As modern-day technology is being used in the world, therefore, modeling multiphase flow systems through CFD simulation can save material setup costs to perform experiments in labs and can reduce the long human hours of work.

CHAPTER 2 LITERATURE REVIEW

2.1. Background

The demand for environmentally friendly production methods has increased as oil costs have risen on the global markets. Transporting fluids upstream and downstream through the pipelines results in major costs because substantial electricity is consumed to operate compressors/pumps to flow the fluids through the pipelines. Different kinds of fluids such as crude oils, gases, and many other liquids are produced from offshore and onshore reservoirs which are then transported through the pipelines to the target facilities. All the fluids adopt different flow patterns during their flow which mainly depend on their physical properties, flow rates, pipe diameter, and inclination of the pipelines [47].

These all fluids are then transported to the target facilities so that they can be further processed and stored. During their process, these fluids are moved through pipelines. Pipelines are transport materials, and they have different kinds of fittings and bends involved in their way. Therefore, when fluids move through the pipelines, they pass through different bend angles which change the flow orientation. These bends can amend the flow behavior and result in an increased pressure drop.



Figure 2.1: Pipeline with different types of Bends

Fluids can flow in the pipelines in different phases which can be single phase, two phases, and three phases. And every flow encounters different kinds of problems. Pressure drops and liquid holdup are the major problems that arise in multi-phase flow systems. However, liquid-oil-gas flow systems are more difficult and complicated than other flow systems. It has more problems as compared to remaining flow systems such as corrosion and erosions which decrease the life of the pipes, and reduction in the fluid's flow rates because of increased pressure-drop and liquid holdup. [48]

1.8. Flow Patterns

Based on numerical and experimental work, several research was carried out to explore the patterns of flow for one or 2-phase, and three-phase flow systems. Researchers have studied the flow patterns, flow characteristics, and problems such as drops in pressure related to fluid flow at different parameters and conditions. Most of the recent research concentrated on the 2-phase methods either liquid-gas or solid-gas flowing through a 90° bend pipe.

Yaqub et al [49] studied the formation of different kinds of flows (primary and secondary), flow characteristics, flow patterns, and problems associated with them like pressure drop during the fluid within the pipelines having the bend angle of 90° bend. At the 90° bend fitting, the specifics of single-phase and secondary flow creation have been studied [50-52].

Many flow patterns can be developed as a result of 2-phase and multiphase flow structures. The individual phase velocity has been the main reason for developing different patterns of fluid flows. The two liquids, often water and oil, move as a distinct layer or as a liquid combination during the three-phase flow. When flowing as combined one flows as a dispersed, whereas the second one is a continuous phase but at interface, in the shape of bubbles, the first one coexists with the later one. The gas-liquid phase adopts different flow patterns due to their different interface relation. The various velocities of water and oil determine the flow patterns of a liquid-liquid system. Therefore, the relationship between liquid-liquid and liquid-gas flow structure is very significant which classifies patterns of 3-phase flow [53]. Liquid-liquid/liquid-gas phases have discrete classifications of flow patterns mainly depending on their interface relationship. And they adopt different flow patterns at different orientations such as they have different flow patterns during straight and vertical pipeline flows. As a result, different researchers have utilized several nomenclatures to describe their flow patterns at different orientations.

2.2. Types of Flow Patterns

Horizontal pipe flow often exhibits one of five distinct patterns: annular flow, slug flow, bubbly flow, plug flow, and stratified flow. When passing through the bends then all straight flow patterns are present with the addition of churn flow and conversion of stratified flow pattern to stratified wavy. These all-flow patterns are developed at different superficial velocities of the phases [47].

2.3.1. Horizontal Three-Phase Flow Patterns

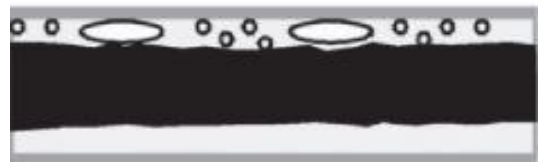
2.3.1.1. Bubbly Flow

A bubbly flow is produced by the dispersion of tiny bubbles of gas throughout the liquid [30]. When different small gas bubbles and one or more small drops of liquid get dispersed into each other during the liquid continuous phase, then the creation of bubbly flow happens which can either be of water-based or oil-based bubbly flow patterns. Various patterns of flow are reported by Bannwart et al [30] having several oil-water relationships. Three-phase patterns of bubbly flow are illustrated in Figure 2.2. Oil-water separate layer flow pattern is evident in Figure 2.2 (a), where bubbles of gas are split up all through a thin layer of water in the pipeline's upper segment. Figure 2.2(b) illustrates the annular flow having water-oil as a core with the dispersion of the bubbles of gas within the higher water film. Figure 2.2(c) illustrates the scattered droplets of oil of numerous volumes in the water segment and gas bubbles demonstrate the irregular oil within the patterns of water flow.

(a) A bubbly flow with distinct films of water and oil



(b) Bubbles of gas in an annular flow have a water-oil core.



(c) Bubbles of gas in a continuous water phase with intermittent oil

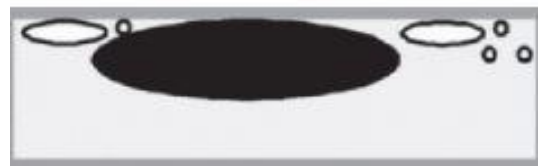
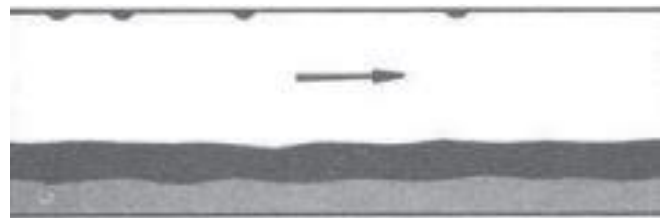


Figure 2.2: Three-phase bubbly Gas-Liquid-Liquid flow patterns [47]

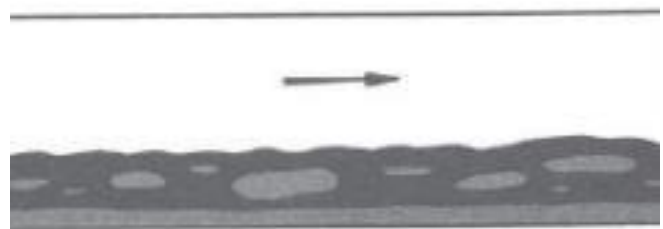
2.3.1.2. Stratified and Stratified Wavy Flow

Based on density, the gas with the lowest density rises to the pipe's top, while oil travels down the center and meets the gas phase at an interface. Two liquids move along in distinct layers each time, oil being lighter than water flowing upper and water being heavier flowing at the bottom. This creates a stratified flow pattern between two liquids. The distinct layer of water and oil during stratified flow patterns is shown in Figure 2.3 (a). Upon raising the gas's flow rate, however, the liquid-gas contact starts to waver. Consequently, a stratified wave-like flow pattern is created. Additionally, when the gas's velocity increases, the turbulence that exists between the two liquid phases also grows, which results in an increase in the amount of mixing that occurs between the liquid phases. Therefore, stratified wavy patterns of flow are created between two liquids. Increasing any liquid phase's volumetric phase fraction will cause that phase to become more preponderant as a continuous phase in overall liquid [54-57]. Figures 2.3 (b) and (c) depict the stratified wavy flow patterns for both oil- and water-based systems respectively.

(a) Stratified flow of distinct water, oil, and gas layers.



(b) Stratified wavy oil based.



(c) Stratified wavy water based.



Figure 2.3: Stratified three-phase flow patterns of Gas-Liquid-Liquid [47]

2.3.1.3. Plug Flow

If the gas flow rate is low and the liquid's is high, then the liquid will act as a driver. Due to its rapid velocity, the liquid is confined to the top center region of the pipes. It is called a plug flow when the gas phase moves as a plug structure while being encased by the fast-moving liquid [19].

The plug flow having separate water and oil layers has been declared by Lee et al [22]. As illustrated in Figure 2.4 (a), the oil phase envelops the gas bubbles in the higher segment of the pipe, while the water film runs independently within the lower segment. Acikgoz et al [23] reported the foam-like appearance of oil-based dispersed plug flow as described in Figure 2.4 (b) while water-based dispersed plug flow was reported through Spedding et al [25] and Figure 2.4 (c) often shows gas bubbles clustered around the gas voids.

(a) Distinct films of water and oil in plug flow



(b) Plug flow based on oil.



(c) Plug flow based on water.



Figure 2.4: Plug three-phase flow patterns of Gas-Liquid-Liquid [47]

2.3.1.4. Slug Flow

The highly typical pattern of flow for liquid-gas exists as slug flow. It is the opposite of plug flow, and according to Acikgoz et al [23] instead of liquid, gas drives the liquid phases in slug flow. When the tiny bubbles of gas combine and shape into a big bubble known as the Taylor bubble, they convert their sharpness into an irregular-shaped bubble. Hence shift the plug flow to slug flow [17, 19].

There are two types of liquid-liquid flow: water-based and oil-based. The oil-based separated slug flow reported by Spedding et al [25] is depicted in Figure 2.5 (a), where water with scattered oil droplets flows in the pipeline's bottom section and is covered in an oil layer. They stated that a liquid mixed coating is present on top of the gas bubbles at the pipeline's upper cross-section. The liquid from the film constantly flowed downhill at the gas-liquid contact, creating a structure resembling a wave.

Along with the slug flow, a uniform mixture of oil and water was recorded. Similar to the water-based plug flow, the oil drops encircle the gas bubbles within the water-based slug flow. The mixture of oil-based has also been shown to have a smooth, foam-like fluid structure. The slug flows based on oil and water are depicted in Figures 2.5 (b), and (c) respectively.

(a) Separate oil-water layers in Slug flow



(b) Slug pattern based on oil.



(c) Slug pattern based on water.



Figure 2.5: Slug three-phase flow patterns of Gas-Liquid-Liquid [47]

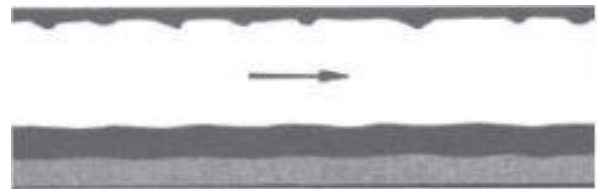
2.3.1.5. Annular Flow

There is also the phenomenon of annular flow in three-phase flow systems when vertical flows are involved. In this, both liquids have separate annular layers, or both liquids present as a mixture that encases the gas moving through the pipe's center [30, 58].

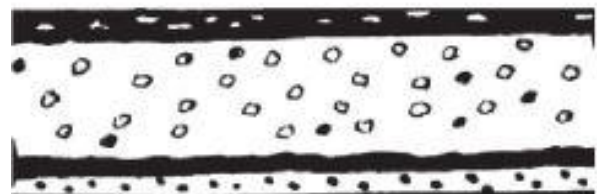
During larger gas velocity, the gas and liquid phases flow within the annular zone and core of the pipeline. As a result, liquid encloses the gas on all sides. Shumueli and Unander et al [59], Lee et al [22], Wang et al [60], Acikgoz et al [23], Spedding et al [25], Wu et al [61], Wegmann et al [62], and Hu et al [63] reported the annular flow. The varying degrees of relationships have been observed in the annular flow of liquid phases. In the pipeline's lower cross-section, during the flow of the annular with a distinct water-oil film, the annular liquid was made up of a layer of oil that covered the water film at the pipe's bottom.

Water has higher density as compared to the other two phases, its layer exists only at the pipeline's lower cross-section, while as illustrated in Figure 2.6 (a), the oil sheet was only present in the pipe's upper cross-section during the annular layer. The gas dispersed in the annular flow of liquid combination is surrounded by the annular layer of oil-water mixture. Figures 2.6 (b) and (c) depict the liquid mixtures for gas-liquid annular flow that are based on oil and water, respectively.

(a) Distinct layers of water and oil during the flow of annular



(b) Flow of Annular based on oil



(c) Flow of Annular based on water

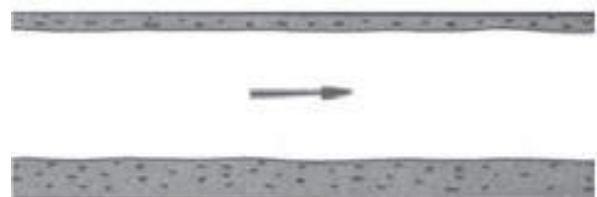


Figure 2.6: Annular three-phase flow patterns of Gas-Liquid-Liquid [47]

2.3.2. Flow Patterns of Three-Phase Flow in Vertical Orientation

In the 3-phase flow, straight horizontal and upright flow patterns exist distinct from one another. The most common patterns of liquid-gas three-phase flow that were observed include churn, bubble, annular, and slug flows. When comparing vertical 3-phase flow versus horizontal 3-phase flow, a notable difference has been found in the liquid-liquid connection. This section provides a quick overview of the vertical three-phase flow structure.

2.3.2.1. Bubbly Flow

Pietrzak et al [58], Liu et al [64], Xie et al [65], Geo et al [66], and Geo and Jin et al [67] have reported the vertical bubbly 3-phase flow. During vertical bubbly 3-phase flow, one liquid phase droplet and bubbles of gas are distributed all through the liquid continuous phase. Figure 2.7 illustrates several water-based and oil-based bubble flow patterns. The water and gas bubbles are dispersed during the bubbly oil-based flow as described in Figure 2.7 (a). The blackish brown flow coloration suggests the oil based. Figure 2.7 (b) shows that the oil bubbles can be distinguished from gas bubbles while the flow turns into water based.

The oil plug that flows through the pipeline's core section is accompanied by gas bubbles as illustrated in Figure 2.7 (c). Big gas foams are made by coalescing the gas bubbles with one another whenever the gas velocity has escalated. That's where, as Figure 2.7 (a) illustrates, bubbly flow changes to slug flow.



a) Bubbly oil-based flow

b) Bubbly water-based flow

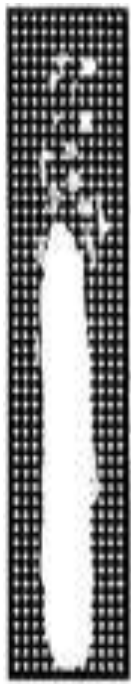
c) gas bubbles and oil plugs in a water-based solution.

Figure 2.7: Vertical bubbly three-phase flow patterns of Gas-Oil-Water [47]

2.3.2.2. Slug Flow

It has been noted that the oil droplets congregate around the gas bubbles next to the liquid-gas interface. The dispersed slug flows based on water and oil are depicted in Figures 2.8 (a) and (b). In the annular zone, as in the oil slug flow of water-based, the majority of the water flows next to the wall, and were stated by Woods et al [31] and Bannwart et al [26]. Taylor bubble and oil were streamlining through the pipeline's core intermittently. Thus, in the case of transferring heavy oil, this kind of flow, in which the water layer functions as a lube involving oil and the wall, the gas bubbles within the oil create a lift against gravity, is highly advantageous.

Figure 2.8 (c) shows the oil slug flow of water based.



a) Flow of slug having dispersed Oil



b) Flow of slug having dispersed water



c) Flow of slug based on water.

Figure 2.8: Vertical Slug three-phase flow patterns of Gas-Oil-Water [47]

2.3.2.3. Plug Flow

The plug flow pattern does not occur very frequently when the three-phase flow is flowing in the vertical direction. Pietrzak et al [58] reported the plug flow patterns having water- and oil-based. A narrow film of liquid with the pipe's internal wall made up of an oil-based mixture was noticed during the plug flow of oil-based. Figure 2.9 (a) shows the liquid and gas plugs flowing to be intermittent. The scattered oil droplets inside the water phase have been shown in Figure 2.9 (b) during the plug flow of water-based, however, it has been noted that there is more turbulence in the liquid mixture flow than within the flow based on oil.



(a) Flow of Plug based on Oil



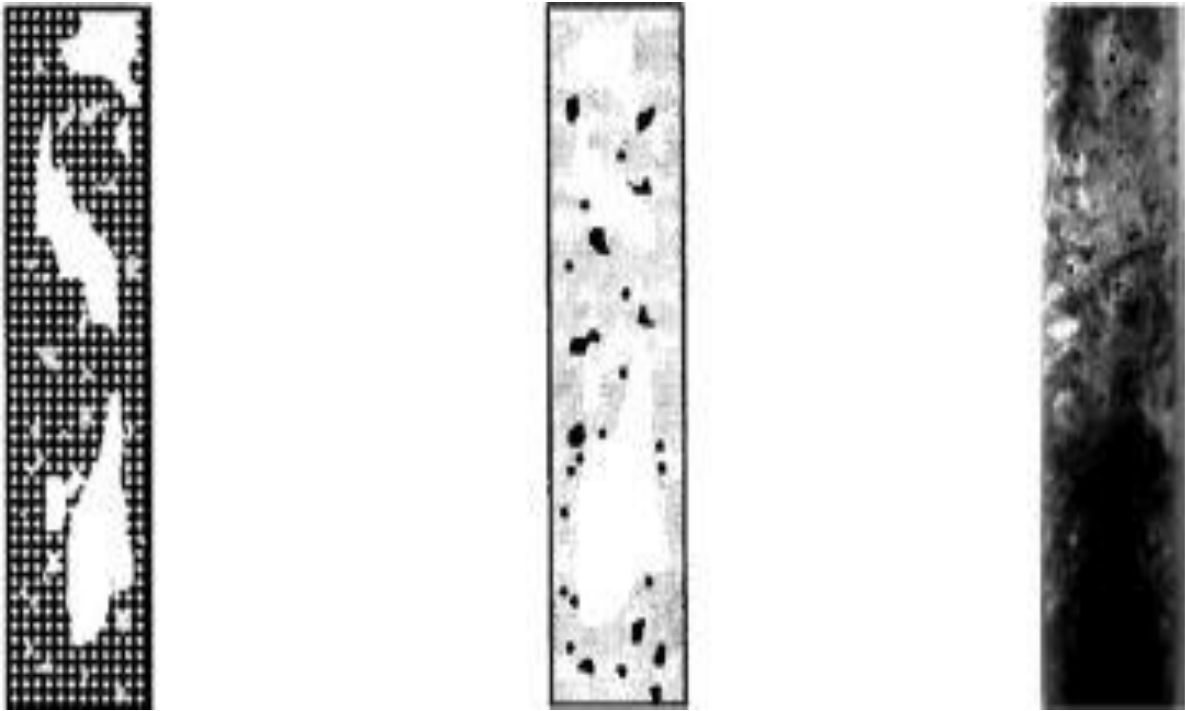
(b) Flow of Plug based on water

Figure 2.9: Vertical Plug three-phase flow patterns of Gas-Oil-Water [47]

2.3.2.4. Churn Flow

Churn flow patterns are observed barely in upright flows in three-phase flows. If gas is traveling at a quicker rate than related to the liquid, bubbles of gas will rise above the fluid. This phenomenon continues until the film of liquid is torn up by the bubble of gas and spreads alongside the walls of the pipe. Oscillatory motion is produced when the liquid phase is drawn down the pipe's walls by gravity. This is called Churn flow [30, 64, 68, 69].

Spedding et al [32], Wang et al [70], Liu et al [64], Bannwart et al [26], Woods et al [31], and Wang et al [68] reported churn flow during vertical 3-phase flow orientation. The pulsating characteristic of churn flow prevents it from having a distinct flow structure as reported by Bannwart et al [26]. Once the two liquids are fully combined, the characteristics of the 2-phase and 3-phase churn flows are comparable as stated by Woods et al [31]. The flow patterns of churn based on oil and water are depicted in Figure 2.10(a) and (b). The scattering of heavy oil in the liquid phase granularly is illustrated by Figure 2.10 (c). The reason is that there is a transition of the ruptured Taylor bubble into churn flow as reported by Liu et al [64].



(a) Flow of churn having dispersed Oil

(b) Flow of churn having dispersed water

(c) Transition of Churn flow

Figure 2.10: Vertical Churn three-phase flow patterns of Gas-Oil-Water [47]

2.3.2.5. Annular Flow

During vertical 3-phase flow, the most observed flow pattern is the annular flow. Bannwart et al [26], Pietrzak et al [58], Woods et al [31], and Spedding et al [32], stated patterns of annular flow of 3-phase in a vertical orientation. In the course of vertical annular flow, liquid mix encircles the gas that flows in the pipeline's core or as distinct annular layers of both liquids. Figures 2.11 and 2.12 show the collaboration of water and oil in various ways with each other.

Two categories of continuous oil annular flow were reported by Woods et al [31], one with two types of annular layers in the first kind, and an oil-based cracked annulus in the second. In the first type, the water droplets are distributed throughout the oil phase, forming an oil-based annular layer that sits on top of the oil annulus layer within the pipe wall. In the second type, when water velocity increases,

water-based layers take the place of oil-based annulus film. The oil annulus film delaminated results in a hard marble structure look. Figure 2.11 (a) and (b) show the annulus flows with oil based.

Woods et al [31] have observed the two types of water-based annular flows. A boundary between an annular film of oil and an annular water layer makes up the first type. As the gas velocity is raised oil drops are distributed within the film of annulus water, as seen in Figures 2.11 (c) & (d), which reveals the rippling and rolling are produced over the oil and gas interface. Two distinct annular layers of liquid combine to form a single annular layer when the water drops are dispersed completely into the oil because the turbulence has been increased in the liquid due to the high gas flow rate.

Figure 2.12 (e) & (f) shows similar annular flow of water-based and oil-based reported by Spedding et al [32]. At minimum pressure drop, the transportation of oil with high viscosity has been emphasized by Bannwart et al using Core Annular Flow (CAF). A flow annular with high oil velocity was found, containing both water within the annular region and oil in the core. While, in the water phase, there were gas bubbles dispersing. Figure 2.12 (g) depicts that water film within the core provides the lubrication for the oil phase which makes the transportation of the oil cheaper and economically sustainable.

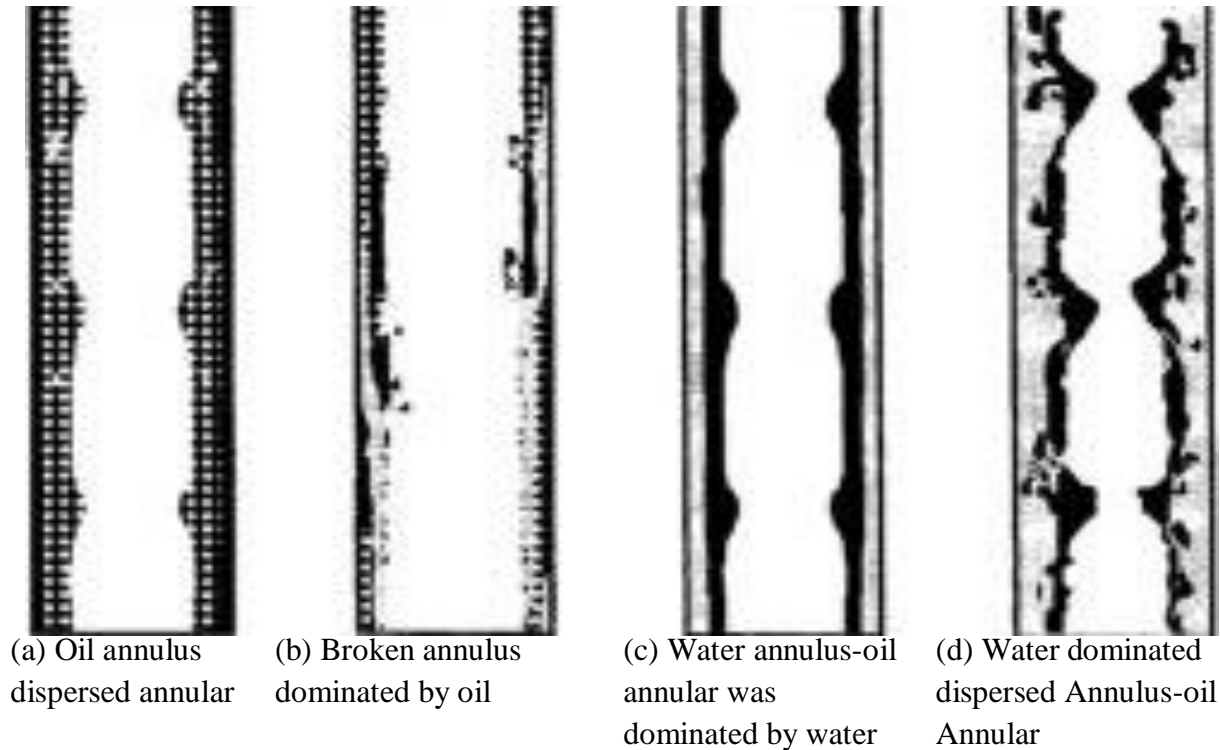
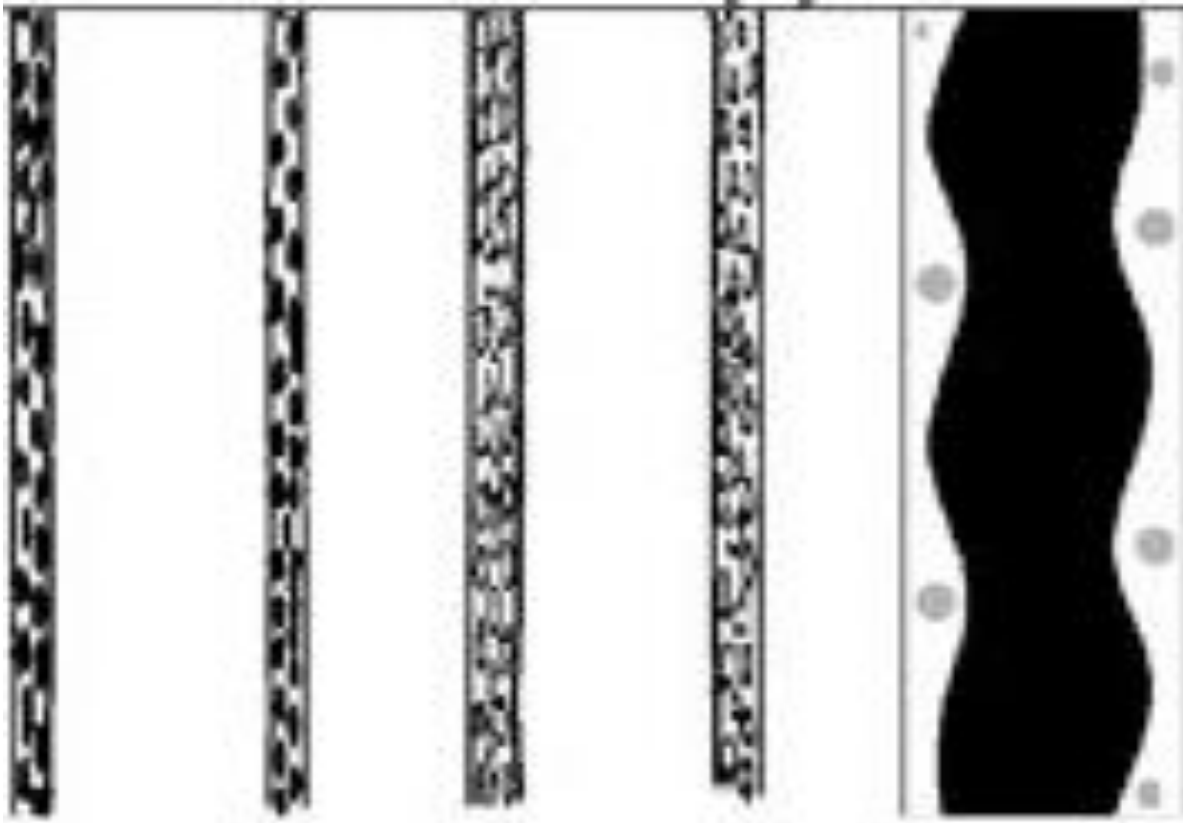


Figure 2.11: Vertical core-annular three-phase flow patterns of Gas-Oil-Water [47]



(e) Dispersed annular oil-based flow (f) Dispersed annular oil-based flow (g) Annular oil-water core flow having gas bubbles within water.

Figure 2.12: Vertical core-annular three-phase flow patterns of Gas-Oil-Water [47]

2.4. Multiphase Flows

2.4.1. Two-Phase Flow

2.4.1.1. Experimental Literature on Two-Phase Flows

Numerous studies have been directed on the 2-phase flow pattern of liquid-gas and water-oil in a curved pipeline, in addition to the flow patterns it produces and other considerations. Wang et al [71] experiments involving 2- and 3-phase flows that were either steady or transient were investigated. There have been several different proposals made for angular flow patterns for 2- and 3-phase flows. Research utilizing oil-water 2-phase flow has been analyzed to determine the patterns of flow that occur in inclined and horizontal pipelines. It was suggested by Rodriguez et al [72] that a flow patterns map that depends on angle be created. Across a vertical conduit, a 2-phase flow of liquid-liquid fluxes was explored by Jana et al [73]. The Core-Annular Flow, also known as CAF, was discovered to be present when the kerosene velocity was high, but the water velocity was low. Churn turbulent flow patterns have also been reported when an intermediate region is created between bubbly and annular flow. This intermediate region was characterized when the two liquids were randomly distributed with changing interfaces.

Ghajar et al [74] focused experimentally on the patterns and characteristics of the flow of non-boiling 2-phase flow within the parallel orientation and in a gradually sloped pipeline. They proposed that the flow patterns, inclination angle, and Reynolds numbers of superficial gas/liquid were extremely main reasons on which the heat transfer results depended. Sotgia et al [75] examined the 2-phase flow pattern of water and oil within the straight pipelines experimentally. They have examined the continuous flow of water and oil in two phases using common home water and mineral oil in a horizontal pipeline. The experiment was designed to simulate real-world conditions.

Xu et al [76] explored the properties of phase inversion and frictional pressure gradients on water-oil 2-phase flows in upstream and downstream pipes. Zong et al [77] conducted experiments with a 2-phase flow pattern of water and oil and discovered and advocated various flow patterns for different angles of inclination. They hypothesized that the gradient of the pipeline played an important part in determining the level of mixing that occurred in the system.

During the experimental investigation of upright rising water and oil 2-phase flow, the following types of flows were observed: slug flow water having oil in it, scattered flow water having oil in it, extremely fine dispersed flow with water having oil in it, transition flow, and flow with oil having water in it. All of these flows were presented by Du et al [78].

Al-Wahaibi et al [79] explored the shift of stratified patterns towards non-stratified patterns of flow in water-oil two-phase stream in horizontal pipes due to varying oil viscosity, the internal diameter of the pipe, and oil and water velocities. This was done to better understand how these factors affect the flow patterns. They postulated that the stratified flow would transition into the dual continuous and bubbly flow after the superficial water velocity hit 12 cP of oil viscosity. This was when they believed this would happen. However, after the oil's viscosity was decreased to 6.4 cP, the disparity between the two values became significantly smaller.

1.8.1.1. Modeling Literature on Two-Phase Flows

Dutta et al [80] analyzed the 2-phase flow of water and oil was reproduced numerically within a conduit that was 2 meters long and 0.5 inches in diameter. It was decided that a 3D pipe simulation would be used instead. To carry out the numerical simulation, they made use of both the Eulerian approach and VOF. They claimed that VOF would be the best and most accurate approach to utilize to anticipate flow patterns during water-oil 2-phase flow, and this was among the goals, as well. for which the VOF would be used. Recent research has provided evidence regarding the velocity division and pressure distribution of flow within the circular elbow when it is subjected to turbulence [81-83].

Hu et al [2] examined the flow of liquid and gas characteristics across a cross-sectioned straight to upright 90° bend using the CFD tool and reported the distributions of both pressure and velocity profiles. Several distinct flow patterns are possible, each of which is determined by the characteristics of the fluid as well as the radius of the bend. They have postulated how curvature affects the flow of slug [84, 85].

The limited details of the flow field have been obtained due to the experimental study limitations, for instance, in examining the effects of inclination, many researchers have used numerical methods by using commercial CFD tools [86]. The frequency of flow of the slug relative to time and variation in the void fraction has been investigated by using the CFD tool. For its multiphase simulation, the method used was k- ϵ turbulence and VOF model [11, 87].

2.4.2. Three-Phase Flow

2.4.2.1. Experimental Literature on Three-Phase Flows

Extensive experimental and mathematical examinations on flow patterns of 3-phase flow and the accompanying pressure losses have been carried out all over the world. Yaqub et al [49] directed an experiment to examine 3-phase flow in a parallel pipe that was upright of a 90° bend. The PVC pipe that was utilized in the experiment had a diameter of 6 inches, a length of 4 meters, a bend-to-diameter ratio of 1, and a length-to-diameter ratio that was greater than one. The surface velocities for the gas were set between 0.5 and 5 meters per second, the surface velocities for the oil were set between 0.08 and 0.36 meters per second, and the surface velocities for the water were set between 0.08 and 0.36 meters per second. Various gas-liquid flow patterns, including stratified roll-wave pseudo-slug, stratified, slug flow, and stratified wavy have been observed. In the context of a liquid-liquid flow, different patterns like ObUL-WLB, WbUL-WLB, SOW-MiF, SOW, and ObM/WbM have been identified. Additionally, pressure loss sensitivity is highly influenced by these flow schemes in both liquid-gas and water-oil systems, as well as by the angle of inclination.

Spedding et al [88] have investigated experimentally fluid flow through a vertical upward pipe to a 90° bend angle horizontal pipe. The experimental setup was a Perspex pipeline made up having an ID of 0.026m. Oil, water, and air had a volumetric flow rate of 0.0001, 0.00015, and 0.02 m³/s, respectively during the experiment. They proposed bending drop of pressure data at the vertical tangent leg, horizontal tangent leg, straight vertical pipe, and at various equivalent length-to-diameter ratios and various gas rates.

Yaqub et al [89] examined the upstream horizontal pipe part that was carrying a three-phase flow was investigated to assess the consequence that a 90° curve had over the phase inversion procedure. PVC tubing that was translucent and measured 0.1524 meters in diameter and 4 meters in length was required for this activity. The pipe had an R/d value of 1. In the experiment, they employed water, gas, and oil, each of which had surface velocities ranging from 0.080 to 0.4, 0.080 to 0.5, and 0.5 to 5 meters per second, respectively. They hypothesized that the bend constraints were to blame for the liquid restrain at less gas velocities because the pressure loss was very complex to the volumetric percentages for both liquid and gas phases.

2.4.2.2. Modeling Literature on Three-Phase Flows

Yaqub et al [90] have studied the use of commercial CFD software which was employed to investigate the co-current flow of 3 phases within a straight pipeline. To maintain an accurate record of the volume fraction, the VOF model was utilized. The pipe's internal diameter is 0.1524 meters, and it has a length of 3.5 meters. In the numerical simulations, surface velocities of 0.5-4 meters per second were utilized for gas, 0.08-0.32 meters per second were used for oil, and 0.08-0.32 meters per second were used for water. In the horizontal part, numerous new types of flow were discovered in addition to the stratified, stratified wavy, rolling wave, and plug flows that were already known to exist. Additionally, it was hypothesized that the pressure would decrease as the exterior velocities of liquid and gas increased.

2.5. Pressure Drop Prediction Models

The vast majority of 3-phase flow prediction methods that have been published are merely gas-liquid model extensions. Lockhart Martinelli [91] includes a liquid and gas 2-phase flow multiplier to accurately estimate the pressure drop that occurs between the 2-phases of liquid and gas. It was based on Reynolds Numbers, viscosity ratio of fluids, density, and weight rates. Brauner et al [92] proposed a model that could be utilized to forecast pressure losses in liquid-based 2-phase systems. Poesio et al [93] combined both models Lockhart-Martinelli and Brauner to identify pressure losses of three-phase and named it a hybrid Lockhart-Martinelli-two-fluid model (LM2FM). Dehkordi et al [94] suggested that a mechanical model be used to evaluate the pressure loss that occurs in horizontal straight pipes as a result of the three-phase viscosity of water, gas, and oil.

In addition to standard models for a horizontal pressure drop that are straight, numerous curved variants have also been developed. Chisholm et al [95] hypothesized that there is a connection between the drop in two-phase pressure at the curve and the relationship between the two. A coefficient B was included in the Lockhart-Martinelli multiplier for gas-liquid systems after it had already been changed. It is related to the ratio of R to D as well as the quantity of loss (k). Sookprasong et al [96] constructed a model that was quite similar to Chisholm's in order to estimate the amount of pressure that would be lost around the bend.

CHAPTER 3 METHODOLOGY

3.1 Geometry

The Simulation work has been conducted with two geometries having curvature radii and the (R/d) ratio of 0.1524 m and 1 respectively. The 90° bend and 180° bend pipes with a larger diameter of 6 inches are widely used in the petrochemical industries. Therefore, three-dimensional (3D) geometries of 90° bend with upstream horizontal and downstream vertical pipes and 180° bend geometry have been created in the SolidWorks version 21 software to simulate the flow patterns of 3-phase flow as shown in figures 3.1 & 3.2. The Pipe's internal diameter (ID), and the horizontal and vertical pipe's length are 6 inches, 4 m, and 3 m respectively. The research found that a minimum pipe length to diameter (L/D) ratio of 10 was necessary for a fully developed velocity profile in turbulent flow. Therefore, the newly constructed pipes are adjusted to have an L/D ratio of 23 [97]. This is done so that the flow can be developed farther along the length of the pipe and its variations in features can be studied.

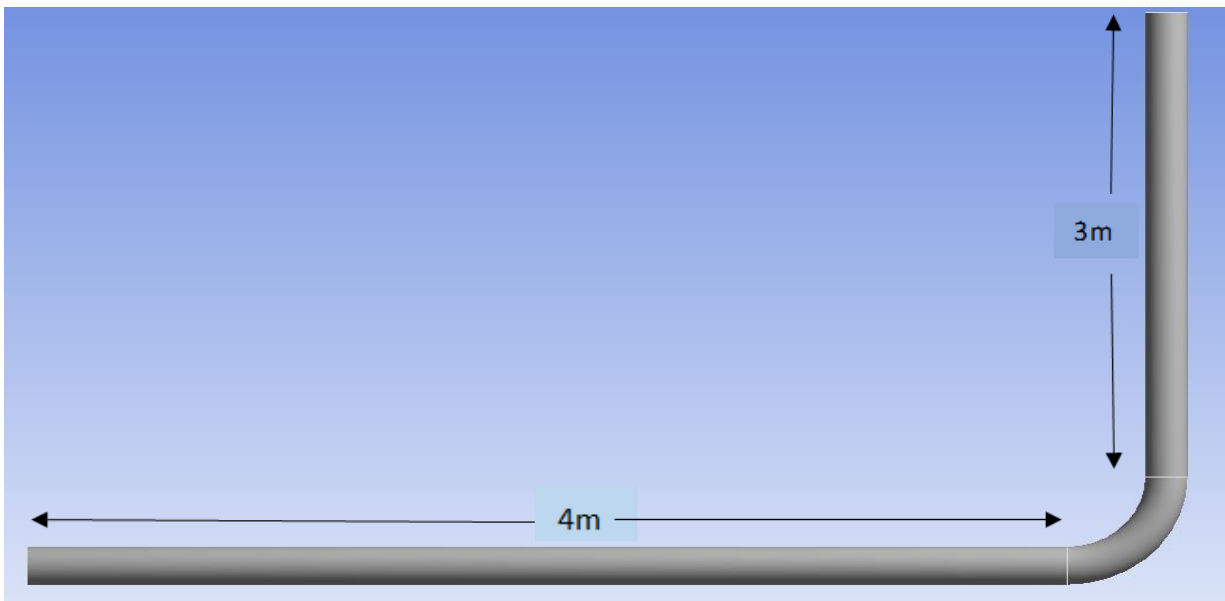


Figure 3.1: 90° bend geometry [5]

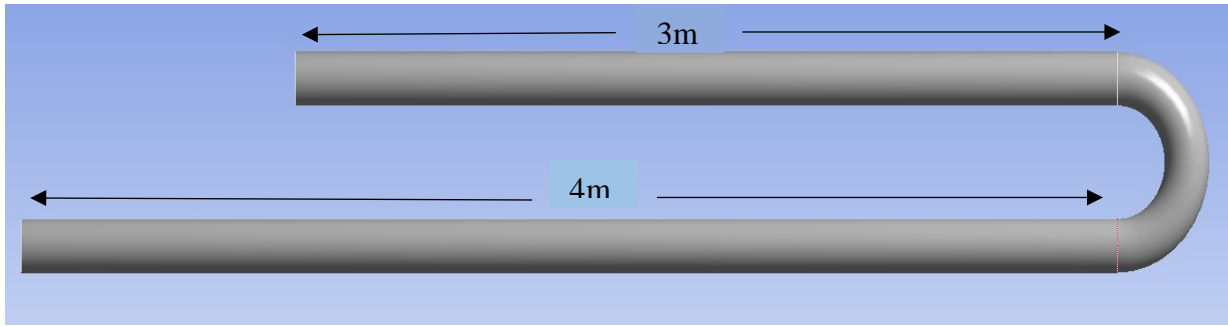


Figure 3.2: 180° bend geometry.

3.2 Meshing

Meshing is done in the CFD ANSYS Fluent 2022R2 software. The results obtained from the CFD assessment are significantly influenced by the choice of mesh used. The hexahedral and tetrahedral were the assembly methods that were available for meshing. The reason for preferring the tetrahedral mesh was the lower skewness and improved orthogonal quality. A fine meshing with lower skewness and improved orthogonal quality has been performed to ensure the quality post results. The maximum total pressure was calculated for each type of mesh by doing a mesh independence analysis with at least six different numbers of mesh cells (as demonstrated in Figures 3.8 & 3.9). This allowed for the calculation of the maximum possible pressure. Figures 3.3 & 3.4 show the meshed geometries of 90° bend and 180° bend pipes.

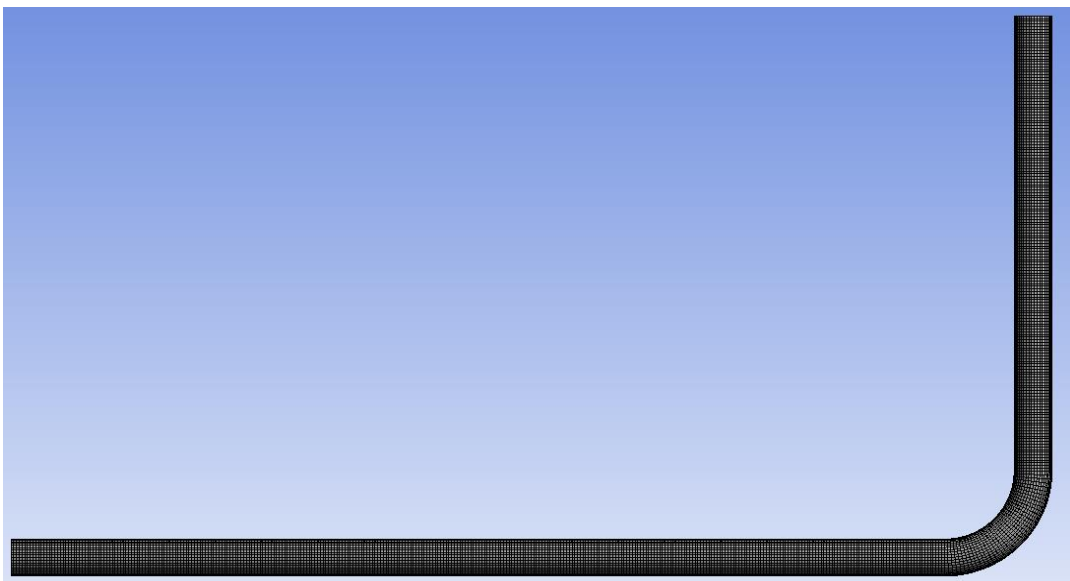


Figure 3.3: Meshed geometry of 90° bend pipe.

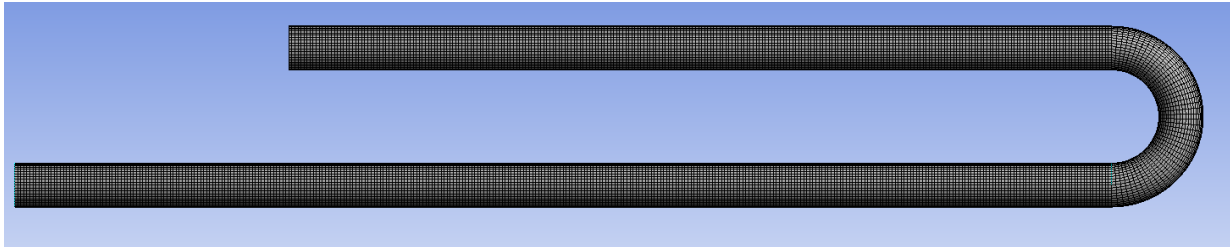


Figure 3.4: Meshed geometry of 180° bend pipe.

Depending upon the maximum and minimum size of the cells, the number of cells in the geometries can be decreased or increased. Because of the approximation over the bigger volumes, the results can be influenced by the lower number of cells. The improved and accurate results can be obtained from the mesh with a higher number of cells, but this will increase the computational cost of the simulation as the number of cells increases. The enlarged straight pipe section and the bends section of 90° bend pipe and 180° bend pipe are shown in Figures 3.5, 3.6 & 3.7 respectively which show a closer view of the applied mesh near the bend and wall.



Figure 3.5: Mesh geometry of enlarged straight pipe section.

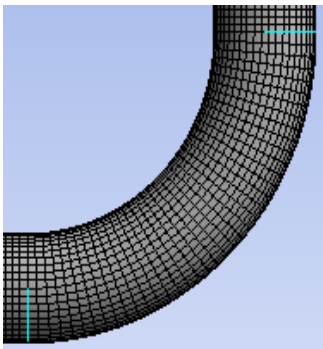


Figure 3.6: Meshed geometry of 90° bend section.

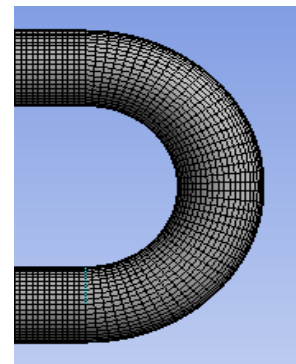


Figure 3.7: Meshed geometry of 180° bend section.

To ensure accurate and consistent results, the number of cells is plotted against the maximum total pressure (Pa). The mesh independence analysis for the geometries of bends 1 and 2 are shown in Figures 3.8 & 3.9.

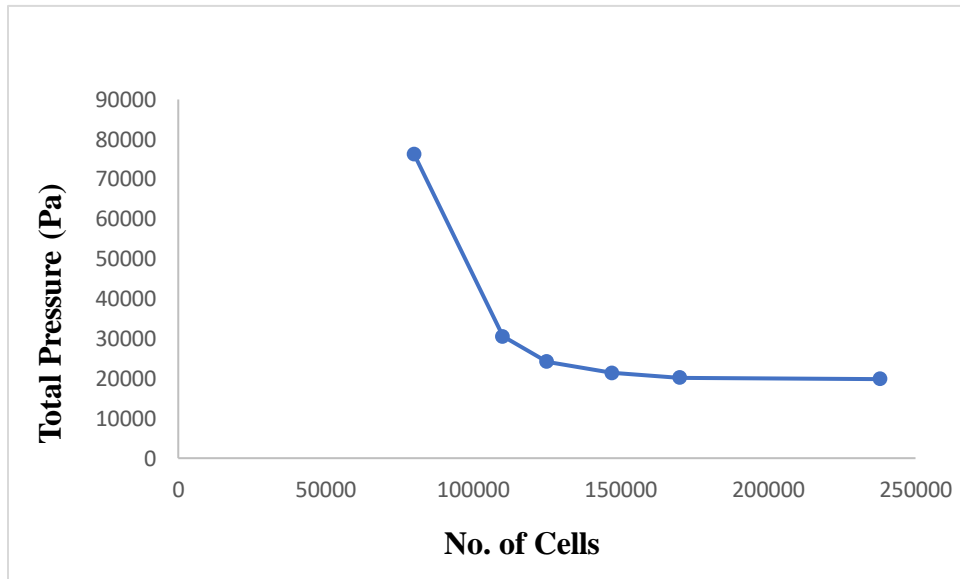


Figure 3.8: Mesh Independence analysis of 90° bend geometry.

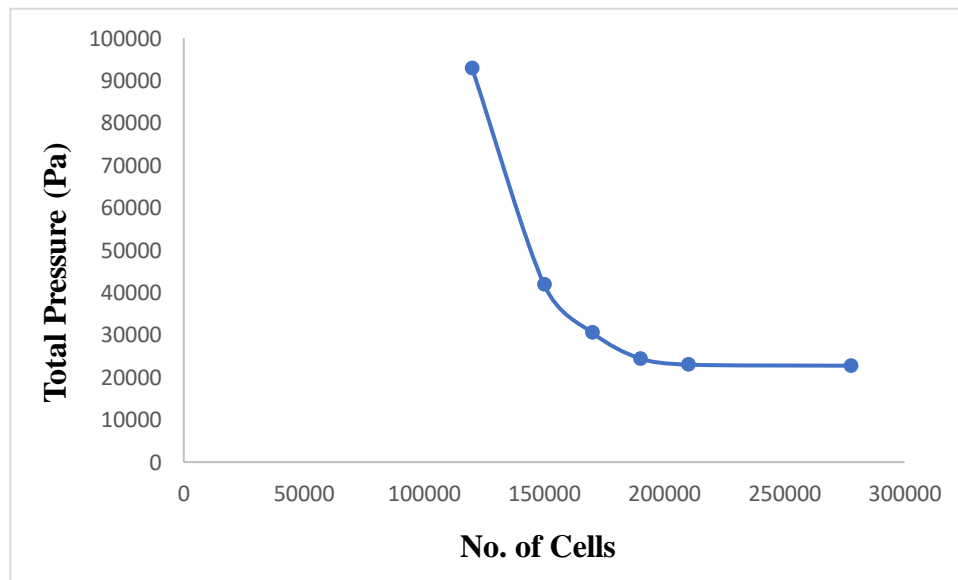


Figure 3.9: Mesh Independence analysis of 180° bend geometry.

The higher quality mesh is very necessary for having accurate and stable numerical computation. Therefore, regardless of the nature of the mesh used, the results of the computation would be very poor if the quality of the mesh is low. For that, before starting the computation process it is very necessary and important to check the characteristics of the mesh. The skewness and orthogonal quality of the cell are the two main important parameters for measuring the quality of the mesh. Both parameters are determined on a scale of 0 to 1. The shape of the cell is very poor if the skewness of a cell is near to 1, and the shape of the cell is excellent if the value is near to 0. For the case of orthogonal quality, a value near 0 shows the worst quality of the cell and a value near 1 indicates the best quality of the cell. The number of cells used for each geometry, orthogonal quality, and skewness of the meshed geometries are given in Table 3.1. The obtained values of the orthogonal quality and skewness of the meshed geometries indicate the very good quality of the meshes.

Table 3.1: Mesh Quality Indicators

Sr. No.	Geometry	No. of Cells	Orthogonal Quality	Skewness
1	90° bend geometry	238044	0.956	0.14
2	180° bend geometry	277604	0.951	0.15

2.6. Multiphase Model

To identify the interfacial relationship between the phases, the VOF model was employed in a multiphase setup. Total number of phases has been set to 3 as three-phase modeling was performed. The flow of immiscible fluids is modeled by working out a set of equations involving momentum. Therefore, the VOF model has the capability to simulate 2 or more non-miscible fluids by only needing to resolve a single group of momentum calculations. Gravitational effect has been included across the flow along the Y-axis by using implicit body forces. As the inertial forces are greater than surface tension forces, therefore, the relevance of surface tension was neglected by Weber number observation [98].

This work is intended to simulate the pressure loss and flow patterns adopted by the three phases, which are highly dependent on the change of volumetric phase fractions with the change in initial flow rates. Regarding this, the VOF model has been selected and was used during the multiphase simulation of 3-phase flow. The VOF model tracks the volumetric phase fraction of the fluids in the whole domain

which enables the model to solve the multiphase flow system by resolving a single group of momentum calculations. In addition, the simulation becomes computationally economical by the single series of momentum formulae. Therefore, for simulating a three-phase flow system, the VOF model was used. Setting up for the VOF model depends upon the flow system under consideration. The two options, the implicit scheme and explicit scheme, are available in the volume fraction parameters. The liquid explicit scheme is used for time-dependent calculations having better numerical accuracy than the implicit scheme. On the other hand, the implicit scheme can either be used with the transient or steady-state solver. However, the scheme is suitable for cases where the intermediate transient behavior is not required. To run the simulation with the transient solver, the explicit scheme was used which allows studying the change in the phase fraction with the movement through the domain. The geometric reconstruction scheme has been used for the volume fraction spatial discretization and the volume fraction cut-off value is maintained at default (1×10^{-6}). For including the gravitational cause during the flow alongside the Y-axis, the implicit body forces have been enabled.

2.7. Governing Equations

The VOF model's momentum equation is as follows:

$$\frac{\partial}{\partial t}(\rho \bar{V}) + \nabla \cdot (\rho \bar{v} \bar{v}) = -\nabla \rho + \nabla \cdot [\mu \cdot (\nabla \bar{v} + \nabla \bar{v}^{-T})] + \rho \bar{g} + \bar{F} \quad (3.1)$$

Whereas, gravitational acceleration (g), phase velocity (v), dynamic viscosity (μ), pressure (p), and density (ρ) are all inputs in this equation. The external force is denoted by the F term and the stress tensor by T .

For one or more than one phase, the equation of continuity for the volumetric fractions has been illustrated:

$$\frac{1}{\rho_q} \left[\frac{\partial}{\partial t} (a_q \rho_q) + \nabla \cdot (a_q \rho_q) \right] = s_{aq} + \sum_{p=1}^n (\dot{m}_{pq} - \dot{m}_{qp}) \quad (3.2)$$

In this equation, ρ and a are the density fraction of q th phase and volume fraction respectively. The S_{aq} is the initial condition, and it always evaluates to zero. Mass is said to be transferred from point (q) to point (p) as expressed in the terms of \dot{m}_{qp} and \dot{m}_{pq} respectively.

2.8. Model of Turbulence Flow

To get accurate results, the simulation of turbulence in the flow is necessary. Because of the high predictive ability of the turbulence model, k -epsilon has been preferred over the other models. The turbulence model of k -epsilon has been proven to be very computationally efficient and numerically robust. As the geometry under consideration is not complicated, therefore the k -epsilon turbulence model has been selected and many multiphase flows and various industrial processes have been simulated by using this turbulence model.

The k -epsilon turbulence model was used during simulation to get accurate post-study results. The flow domain uses flow characteristics that indicate the presence of turbulence when the flow is occurring and uses these characteristics.

The K-epsilon turbulence model is given below:

$$\rho v_j \frac{\partial k}{\partial x_j} = \frac{\partial}{\partial x_j} \left(\frac{\mu_t}{\sigma_k} \frac{\partial k}{\partial x_j} \right) + \mu_t \frac{\partial v_j}{\partial x_i} \left(\frac{\partial v_i}{\partial x_j} + \frac{\partial v_j}{\partial x_i} \right) - \rho \varepsilon \quad (3.3)$$

$$\rho v_j \frac{\partial \varepsilon}{\partial x_j} = \frac{\partial}{\partial x_j} \left(\frac{\mu_t}{\sigma_\varepsilon} \frac{\partial \varepsilon}{\partial x_j} \right) + c_1 \mu_t \frac{\partial v_j}{\partial x_i} \left(\frac{\partial v_i}{\partial x_j} + \frac{\partial v_j}{\partial x_i} \right) - C_2 \frac{\varepsilon}{k} \rho \varepsilon \quad (3.4)$$

Where, the dissipation rate is represented by ε , and turbulent kinetic energy is denoted by k while $\sigma_\varepsilon, \sigma_k, C_1$ and c_2 are the constants.

2.9. Physical Properties and Boundary Conditions of the Fluids

The atmospheric pressure (101.325 kPa) was considered at which the flow system was running, therefore the gauge pressure was operated at zero. For an approach that is more applicable, the appropriate boundary conditions have been chosen which are given below in Table 3.3. At the flow domain's boundary walls, the no-slip requirement was taken into consideration. Table 3.2 illustrates the fluid's physical properties. Phase's superficial velocities and fluid's volume fractions used at the inlet pipe's surface have been calculated. The higher phase fraction of air meant that it was the primary phase, whereas water and oil have been marked as secondary phases. The influence of surface tension is ignored in favor of the more powerful inertial forces as the Weber number climbs above 1. The flow patterns have been examined by simulating at least 20 combinations of all phase velocities. The loss in pressure has also been analyzed by using 2 different kinds of pipe bends.

Table 3.2: Fluid's physical characteristics [5]

Sr. No.	Phases	Density (kgm^{-3})	Viscosity ($\text{kgm}^{-1}\text{s}^{-1}$)
1	Gas (Air)	1.164	1.87×10^{-5}
2	Water	995.71	0.000798
3	Oil	832 at 30 °C	0.00981 at 30 °C

Table 3.3: Boundary Conditions

Mixture velocity range	$0.66\text{-}5 \text{ ms}^{-1}$
Inlet	Velocity Inlet
Pressure	101325 (Pa)
Outlet	Pressure Outlet
Surface Tension effect	Neglected
Gravitational acceleration	Enabled along the Y axis
Wall Roughness (mm)	0.0015
Wall motion	Stationary Wall
Shear Condition	No Slip

3.3 The Time Step and Solver

The multiphase pressure-based solution was employed. To resolve the Navier-Stokes calculations and the momentum calculation, two different methods, the SIMPLE technique, and the second-order upwind strategy were employed respectively. The interface structure shifted over the course of time and has been analyzed between the phases due to the transient calculations. The variable time step of the VOF model proves to be an excellent feature that helps to meet the criteria of the global courant number by modifying the step size by making it smaller or larger in proportion to the increase or decrease in cell size. Courant number has been dimensionless quantity which relates the time stage for the

computation and the characteristics period for the transient of fluid through the control volume given by the equation. This equation is used to calculate the minimum time step for the transient simulations. The highest Courant number accepted for the calculation is decided to be 0.25. The solution has been converged once the residuals are reduced to 10^{-4} . To have complete stability of flow, the simulations run for 8 seconds.

CHAPTER 4 RESULTS AND DISCUSSIONS

4.1 CFD Simulations Results of Flow Patterns in the Bends

Three-phase flow patterns obtained in the 90° bend and 180° bend sections have been successfully modeled in the ANSYS Fluent workbench. The simulation result within the bend section clearly shows the indications of the presence of three types of patterns mainly rolling wave, slug, and pseudo-slug flow patterns. These three types of flow patterns are observed at distinct speeds of the distinct phases. The validation of these patterns observed during CFD simulation results by comparing them with the observed patterns of experimental study is very important and necessary. Therefore, the obtained flow designs of three-phase flow by simulating them in the ANSYS Fluent are compared with experimental work. Three-phase flow patterns observed in the CFD ANSYS fluent matched and exhibited strong conformity to the flow patterns observed in experimental data.

1.8.1.2. Three-Phase Flow Patterns in the 90° Bend

Three-phase flow simulations were conducted within the CFD ANSYS fluent, revealing three distinct flow patterns within the 90° bend section. These patterns emerged at varying superficial velocities and volume percentages of the distinct stages. The observed 3 distinct flow patterns obtained within the 90° bend section of pipe comprised rolling wave, slug flow, and pseudo-slug flow patterns as illustrated in Figure 4.1. The figure indicates that slug flow patterns predominated at lower velocities of the gas phase.

Within the slug flow patterns, water behaves differently than oil arriving in a separate layer, partially mixing, or forming a fully mixed flow. Due to the density differences, the water being the heaviest one flows parallel to the pipe's bottom section, while the oil occupies the pipe's middle section. The density of the gas is the minimum of the other two phases. Therefore, the gas phase being the lightest one flows at the upper topmost section of the pipeline. This occurs because the gas phase's superficial velocity is relatively low during the slug flow. Therefore, there is a small available space for flowing the gas phase within the pipe because the 90° bend section is full of liquid phases.

When the flow rate on the surface of the gas phase is further increased, the slug flow is converted into pseudo-slug flow which usually flows as a separate layer, partially mixing, or forming a fully mixing flow but having a wave during its flow through the bend section. The CFD simulation results clearly show a wave during the pseudo-slug flow pattern within the 90° bend section. The pseudo-slug flow patterns at three disparate surface velocities are given in Figure 4.1. A subsequent rise in the gas phase superficial velocities converted the pseudo-slug flow patterns into rolling wave flow patterns. The rolling wave flow patterns become apparent at higher gas phase superficial velocity as indicated by the simulation results shown in Figure 4.1.

The effects of high gas phase velocity during the three-phase flow system produced the rolling wave patterns which blow the liquid phases in the 90° bend section at the higher gas phase velocity. Owing to the elevated superficial velocities of the phases, both oil and water flow as a blended mixture. Rolling wave flow patterns identified in the simulation analysis of CFD are shown in Figure 4.1.

The comparative analysis of three-phase flow patterns within a 90° bend section between CFD simulation results and experimental work [5] showed good agreement.

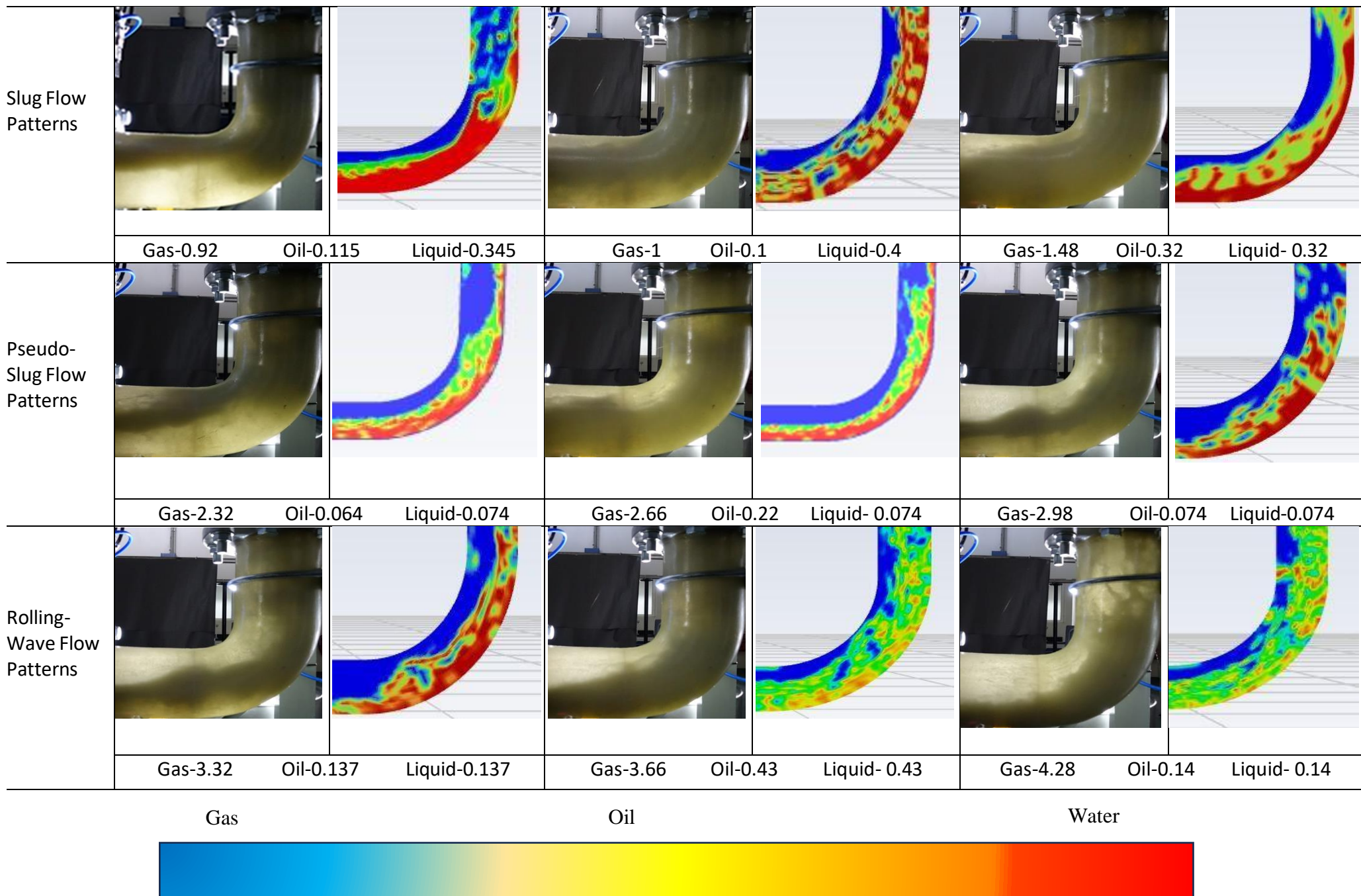


Figure 4.1: Validations of simulation results of three-phase flow patterns in a 90° bend [5]

1.8.1.3. Three-Phase Flow Patterns in the 180° Bend

Three-phase flow simulations have been successfully simulated in the CFD ANSYS Fluent to investigate the flow patterns within the 180° bend pipe. Remarkably, the observed patterns in the 180° bend are the same that were obtained during the 90° bend simulations. These flow patterns included slug flow, pseudo-slug flow, and rolling wave-flow patterns. The slug flow patterns are obtained at low superficial velocities of the gas phase and most of the liquid has been accumulated in the 180° bend section due to the low gas velocity. As the flow passes through the 180° bend section, the liquid flows through the upper section of the bend and gas usually flows through the inner section of the bend. When the flow passed the bend, the liquid phases dropped down on the horizontal section because of gravitational force and gas having less density moved with the upper section of the pipe. During the three-phase slug flow through the bend, the oil and liquid flow as a separate layer, partially mixed or as a mixture. The three-phase slug flow patterns are shown in Figure 4.2.

Slug flows are converted into pseudo-slug flow patterns at subsequent increases of gas phase superficial velocities. The pseudo-slug flow patterns have a wave when flow passes through the bend section. Due to the density difference, the liquid phases fall to the horizontal surface after passing through the bend while gas being the lightest one usually flows at the top section of the pipe. During the flow through the bend, oil, and liquid flow as a separate, partially mixed, or fully mixed flow. The waves are clearly shown in the simulation results of the pseudo-slug movement pattern which are shown in Figure 4.2.

The transition of pseudo-slug flow patterns to rolling wave flow patterns is noticeable at higher gas phase velocities which usually pushes the liquid phases with greater velocity; therefore, the liquid phases are flowing as a mixture flow. Due to the higher gas superficial velocities and liquid, the liquid phases are forced to flow through the outer wall of the bend, and gas flows at the inner wall of the bend. But when the liquid and gas phases pass the bend section, the oil, and waterfall to the line-through section of the pipe gas being the lighter phase flows at the top section of the pipe as a result of the density difference and effect of gravitational forces which pulls the liquid phases down to the horizontal section.

4.2 Pressure Drop Variations in the 90° Bend

With rising gas velocities and an oil-to-liquid volume ratio (f_o) preserved at a steady value of 0.5, the pressure drop from the outcomes of the numerical simulation was examined and contrasted with the experimental data at various liquid surface velocities. With the increasing surface speeds of the liquid and gas, the pressure drop is increasing as shown by the general trend. The flow patterns majorly affect a reduction in pressure across the bends which is also reported in past research work. At the low surface velocities of the gas phase, slug flow patterns have been observed, leading to fluctuations in the pressure drop. Hence, with lower gas phase surface velocities, the pressure abruptly rises and falls. Therefore, the gas phase essentially propels the liquid phase as it travels through the bend with slug flow patterns at a higher velocity.

During the low flow rates, the liquid holdup blocks the gas phase which results in pressure drop fluctuations as shown in Figure 4.3. When the gas velocity phase is increased, the slug flow pattern is converted into pseudo-slug flow, which results in a temporary decrease in pressure losses. The pseudo-slug flow patterns were converted further into a rolling wave flow pattern when the gas phase velocity was further raised. Therefore, pressure drop has been increased with fewer fluctuations previously observed during the slug flow patterns with low gas velocities.

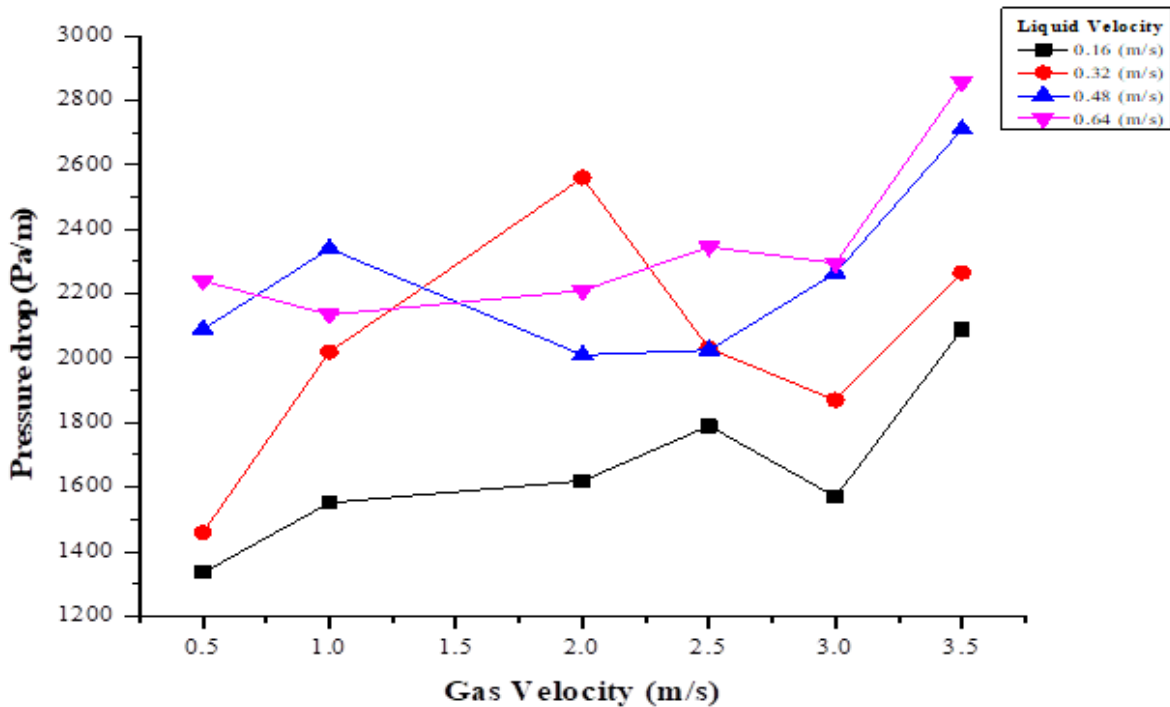


Figure 4.3: Variation in pressure reduction in the 90° bend at a constant f_o value of 0.5 and when the gas and liquid phases' surface velocities increase [5].

At f_o and rising liquid and gas superficial velocities, the overall trend of pressure loss has been examined using experimental data. Figure 4.4 displays the comparison between the pressure drop obtained from CFD and experimental measurements. The comparison graph shows a closely related trend which indicates that the pressure drop values are very close to experimental findings values having a maximum average error of 10.37%.

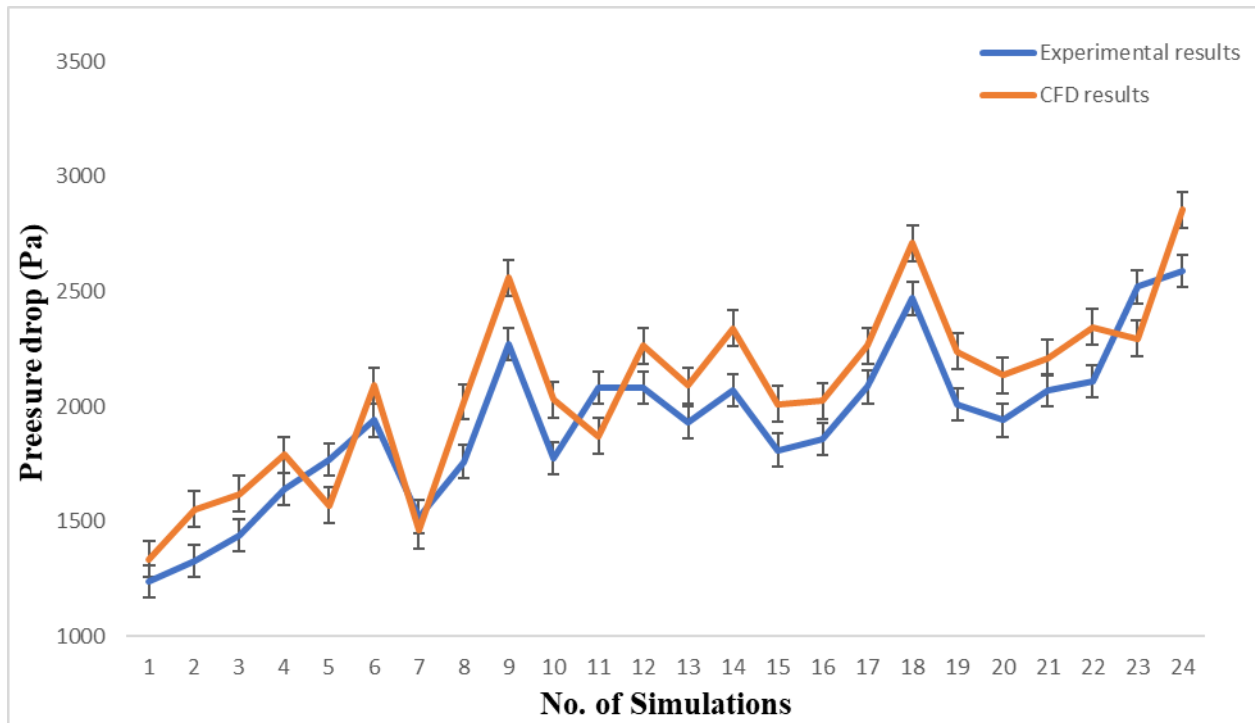


Figure 4.4: Comparison of the CFD results at the 90° bend at a constant f_o value of 0.5 and rising gas and liquid superficial velocities with the experimental findings for pressure drop.

The flow patterns of water and oil have a major influence on the pressure drop in addition to the flow patterns of gas and liquid. As a result, Figure 4.5 illustrates the pressure drop analysis at two distinct f_o , as well as the effects of the continuous liquid phase. It has been maintained that the liquid phase's surface velocity is 0.32 ms^{-1} . When the f_o value is 0.25, the flow is water-based, and when f_o value is 0.75, the flow is oil-based. Variations in the pressure drop and distinct flow patterns have been noted at both f_o values.

The graph's trend unmistakably demonstrates that during the beginning water-based flow, the pressure drop was higher at the low gas superficial velocities; however, when the gas superficial velocities increased, the pressure drop was mostly increased during the oil-based flow. The reason for this is that during an oil-based flow, the pressure loss is greatly influenced by the continuous liquid phase. As a result, it has been shown that the pressure loss during the oil-based flow is significantly higher than during the water-based flow.

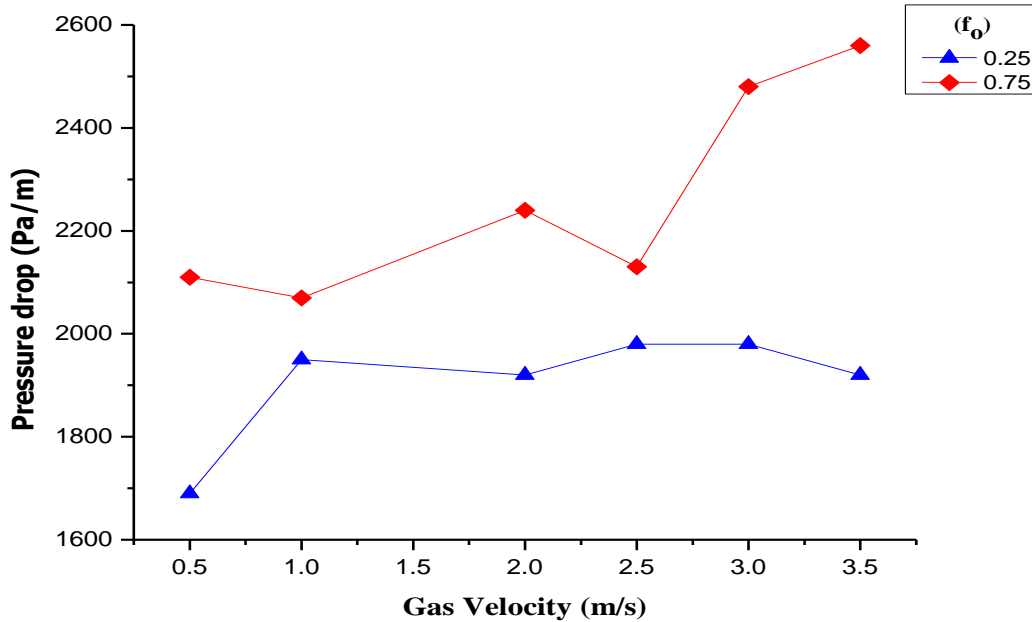


Figure 4.5: Variation in the 90° bend pressure drop with increasing gas and continuous liquid phase superficial velocities while maintaining a constant liquid surface velocity of 0.32 ms^{-1} [5].

As seen in Figure 4.6, the CFD simulation results of pressure drops are compared and evaluated with the experimental results of pressure drops for two distinct f_o values of 0.25 and 0.75. The comparative analysis indicates that the CFD simulation results have a close value with the experimental results having a maximum average error of 12.63%.

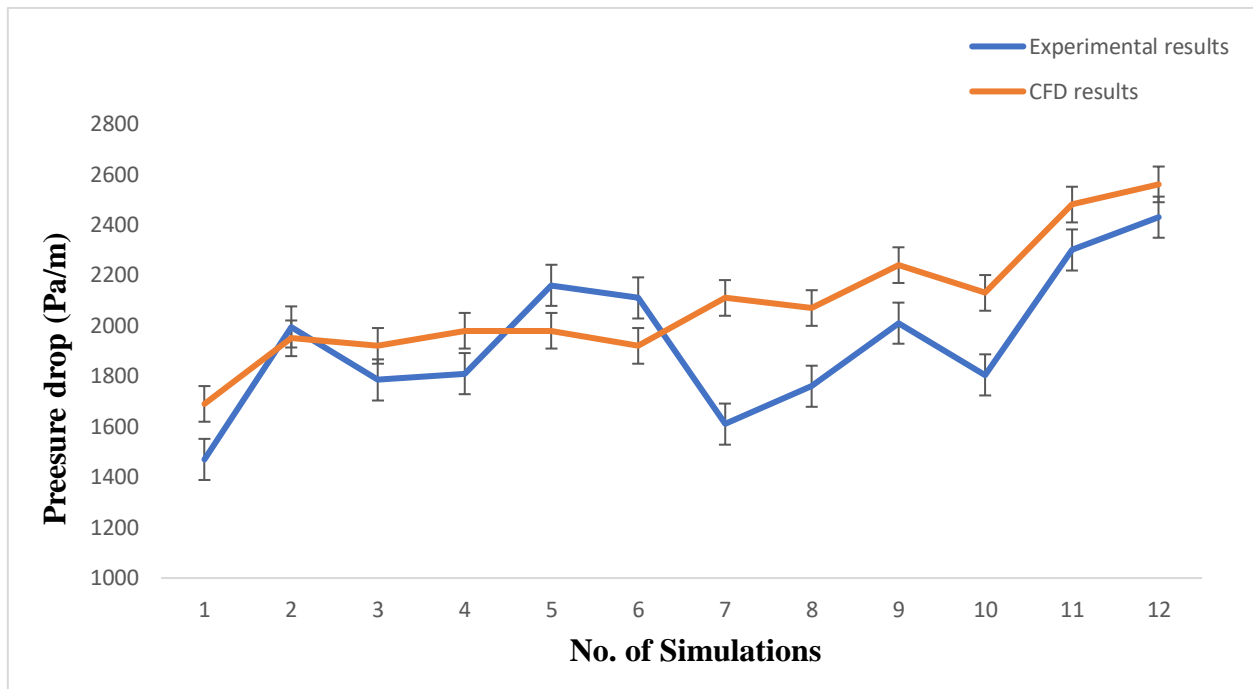


Figure 4.6: Comparison of CFD and experimental pressure drop results in the 90° bend with a constant value of the liquid superficial velocity of 0.32 ms^{-1} with an increasing gas velocity and continuous liquid phase velocity.

Additionally, the analysis and contrast of the pressure drop variation with the findings of the experiment have been conducted at a constant liquid superficial velocity of 0.4 ms^{-1} and an increasing f_o values from 0.2 to 0.8. Figure 4.7 makes it abundantly evident that the pressure drop in the 90° bend exhibits considerable variability and has higher pressure drop values at f_o and low superficial velocities of the gas phase. The flow based on water has been happening at a minimal f_o value, which is the cause of varying pressure drop values in the 90° bend section pipe.

The pressure drop values are near to one another as the f_o rises as gas velocities rise. This is because, during the flow through the bends, the influence of gas lift which becomes extremely substantial at the higher surface velocities of the gas phase reduces the impact of oil-based flow. Consequently,

the pressure drop has larger values but exhibits slight changes at the higher f_o value and higher gas phase superficial velocities, as illustrated in Figure 4.7.

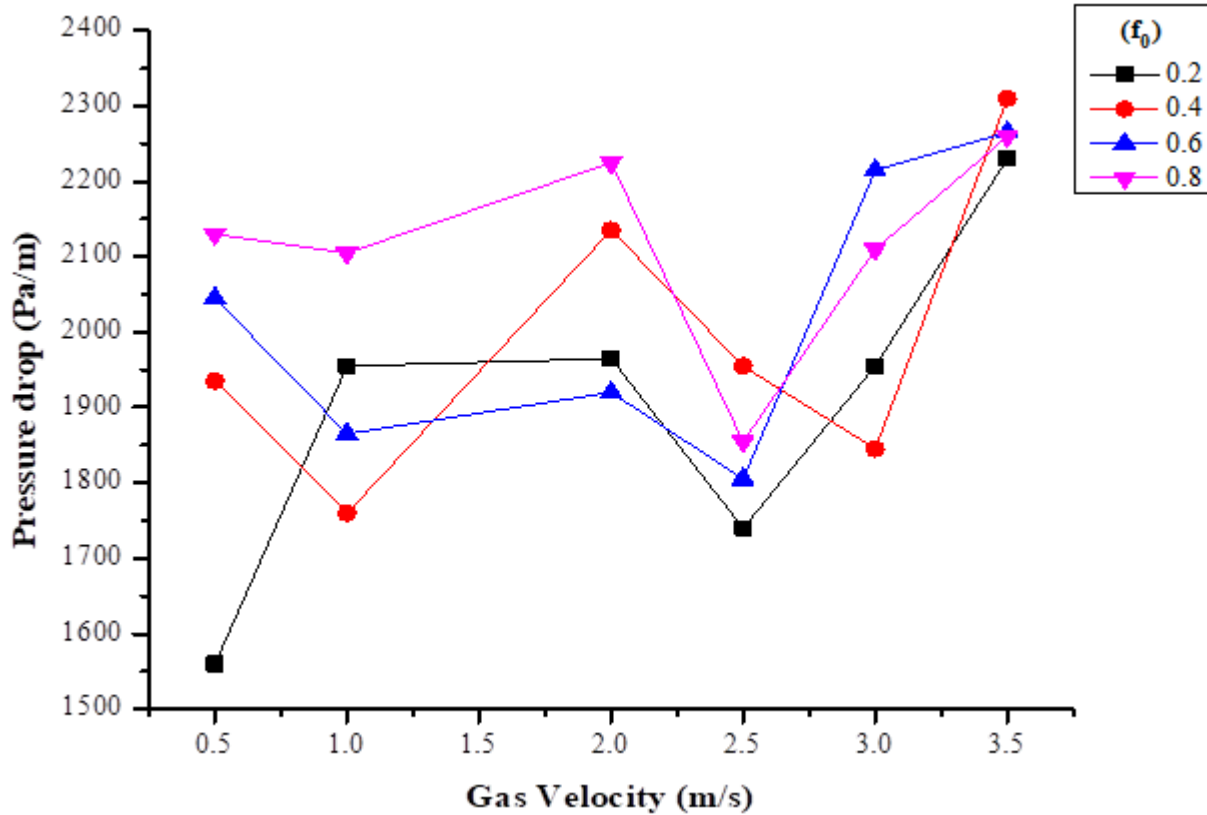


Figure 4.7: Pressure drop disparity in the 90° bend with rising gas and f_o value and a constant liquid superficial velocity of 0.4 ms^{-1} [5]

The pressure drop results of CFD simulation having 0.4 ms^{-1} constant value of liquid velocity and with increasing gas phase superficial velocity and f_o range 0.2 - 0.8 are compared with experimental results of the previous work as shown in Figure 4.8. The Figure clearly shows a similar trend adopted by the CFD simulation results in contrast to the experimental results. It shows that pressure drop results have a close value with the experimental work with a maximum average error of 9.03%

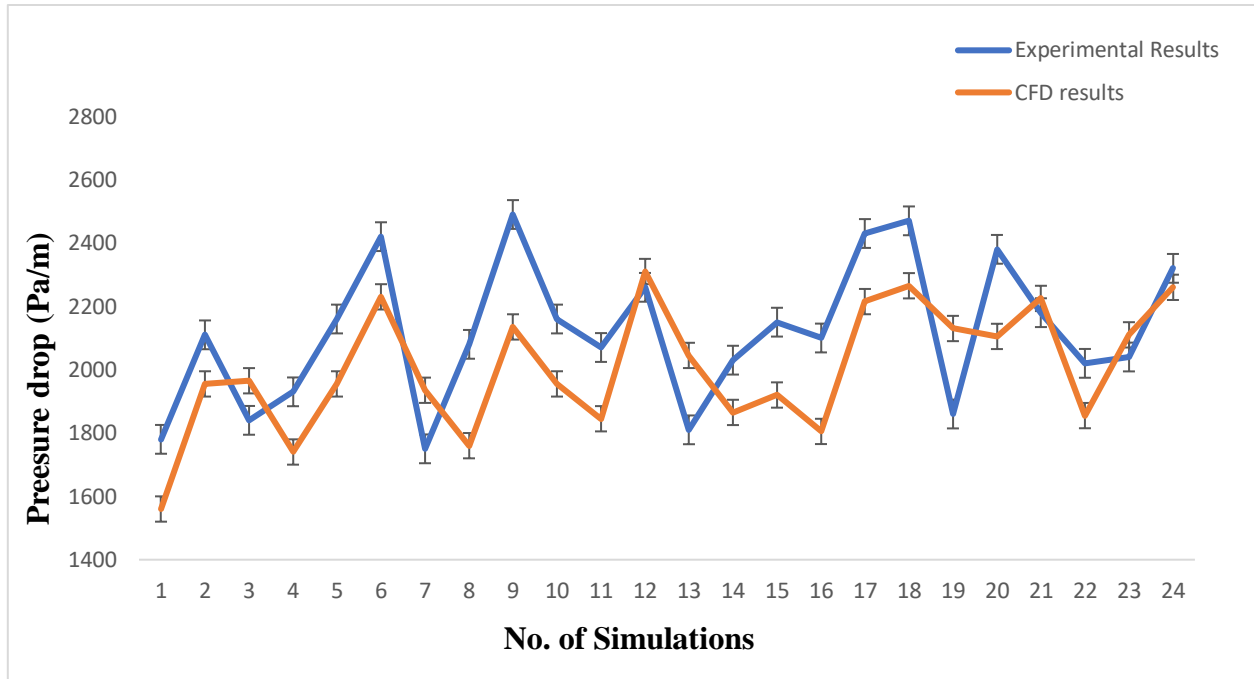


Figure 4.8: Comparison of CFD pressure drop results with experimental results in the 90° bend of a constant superficial velocity of liquid at 0.4 ms^{-1} with an increasing gas velocity and f_o value.

4.3 Pressure Drop Variations in the 180° Bend

With increasing gas and liquid superficial velocities, the pressure loss throughout 180° bend has been investigated while maintaining a constant f_o value of 0.5. Variations within the liquid and gas surface rates, ranging between 0.16 and 0.64 m/s and 0.5 to 4 ms⁻¹, have been simulated. As seen in Figure 4.9, a lower pressure decrease has been seen for low gas superficial velocities than at high gas velocities. As the gas velocities rise even further, there is also a variation. This is a result of the slug flow existing at the gas's low surface velocities. The pressure loss grew as the gas velocities were raised more. The reason for increasing the pressure drop was that the slug flow has been converted to pseudo-slug flow which usually increases the pressure losses.

The pressure drops in the 180° bend in previous research has been reported less as compared to 90° bend. When the trending graph of 180° bend was compared and analyzed with the graph of 90° bend, the pressure drops results of 180° bend were way less than the 90° bend pressure drops. This comparison validates the pressure drop results of 180° bend. The change of pseudo-slug to rolling wave flow patterns at the higher gas velocities has increased pressure drop values when the gas superficial velocities are further raised with the increasing liquid velocities. The greater pressure drops values narrow down and fluctuate less at the higher gas phase superficial velocities. The general trend of the pressure drop results is shown in Figure 4.9, which indicates the lower pressure drop values at the low gas superficial velocities, fluctuations as further gas velocities increase, and higher pressure drop values with less fluctuations at higher gas phase superficial velocities.

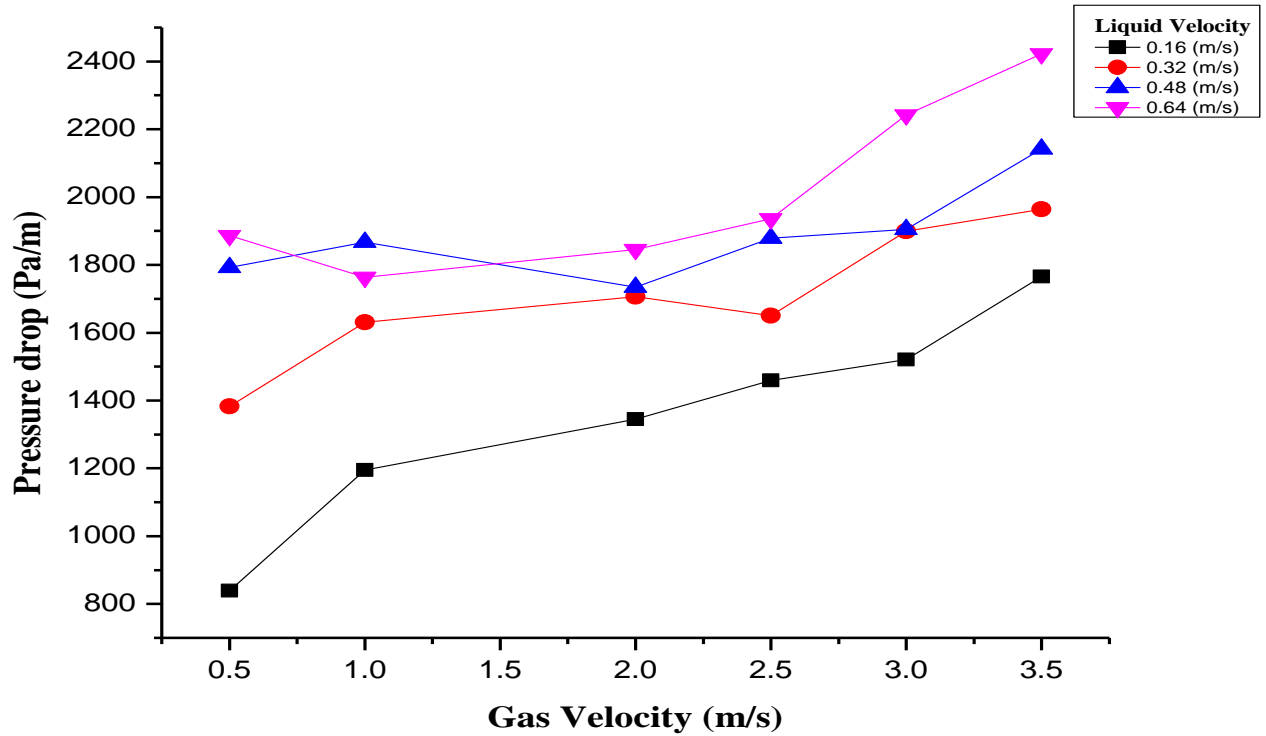


Figure 4.9: Variation in pressure drop in the 180° bend at a constant f_o value of 0.5 with increasing gas and liquid phase superficial velocities.

Moreover, the pressure drop is significantly influenced by the continuous liquid phase. To examine the pressure drops in the 180° bend, two distinct f_o values of 0.25 and 0.75 were used. The water-based flow had a f_o value of 0.75 and the oil-based flow had a f_o value of 0.25. At 0.32 ms^{-1} , the liquid's surface velocity was maintained consistently. Figure 4.10 illustrates the effects of the f_o and the continuous liquid phase at the pressure loss.

Figure 4.10 indicates that the values of pressure drop fluctuated at low gas phase velocities during both cases of water-based flow as well as oil-based flow. But at the higher superficial velocities of gas and during oil-based flow, pressure drop increases significantly. The reason is that there is an oil-based flow, a continuous liquid phase has a major and significant impact on pressure at higher gas phase superficial velocities. By comparing the pressure drop results with 90° bend at two different f_o values of 0.25 and 0.75, the graph shows a little more fluctuation at the low gas phase velocities, but fewer pressure drops values in the 180°.

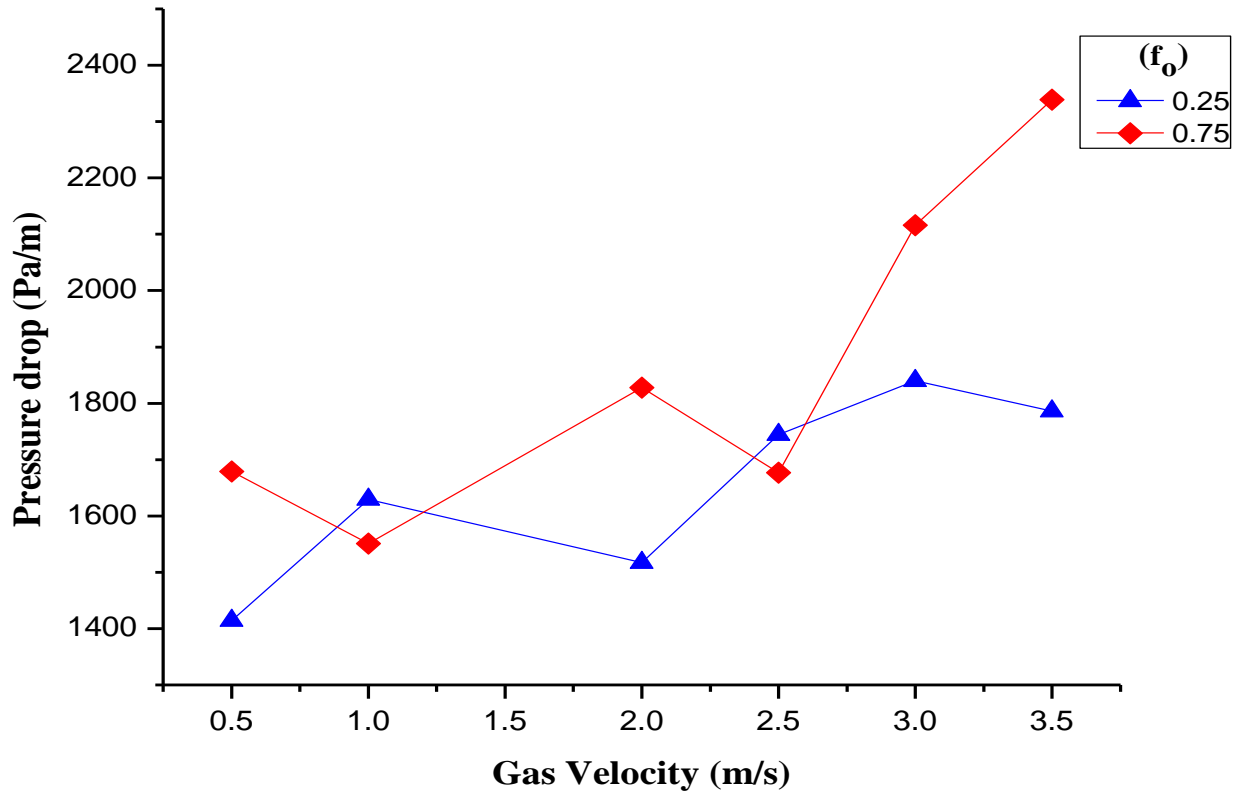


Figure 4.10: Changes of pressure drop within 180° bend at a constant value of liquid superficial velocity of 0.32 ms^{-1} with an increasing gas phase superficial velocity and continuous liquid phase.

Figure 4.11 illustrates the additional analysis of the pressure drop fluctuations at 180° bend at a constant liquid superficial velocity of 0.4 ms^{-1} and rising gas superficial velocities with increasing f_o from 0.2 to 0.8. The figure demonstrates that at low gas surface velocities and low oil-to-liquid volume ratios with notable changes, there have been substantial pressure decreases. The water-based flow at the low f_o value is the cause of these variations. However, the oscillation in pressure drops dropped dramatically and the pressure drop values narrowed down to nearly match each other at greater gas phase flow rates and oil-to-liquid volume ratios (f_o). The reason for this is that during the high surface velocities of the gas, the gas lift greatly affects the oil-based flow. As a result of the diminished influence of oil-based flow, pressure drops in the bend rose, while pressure drop fluctuations decreased.

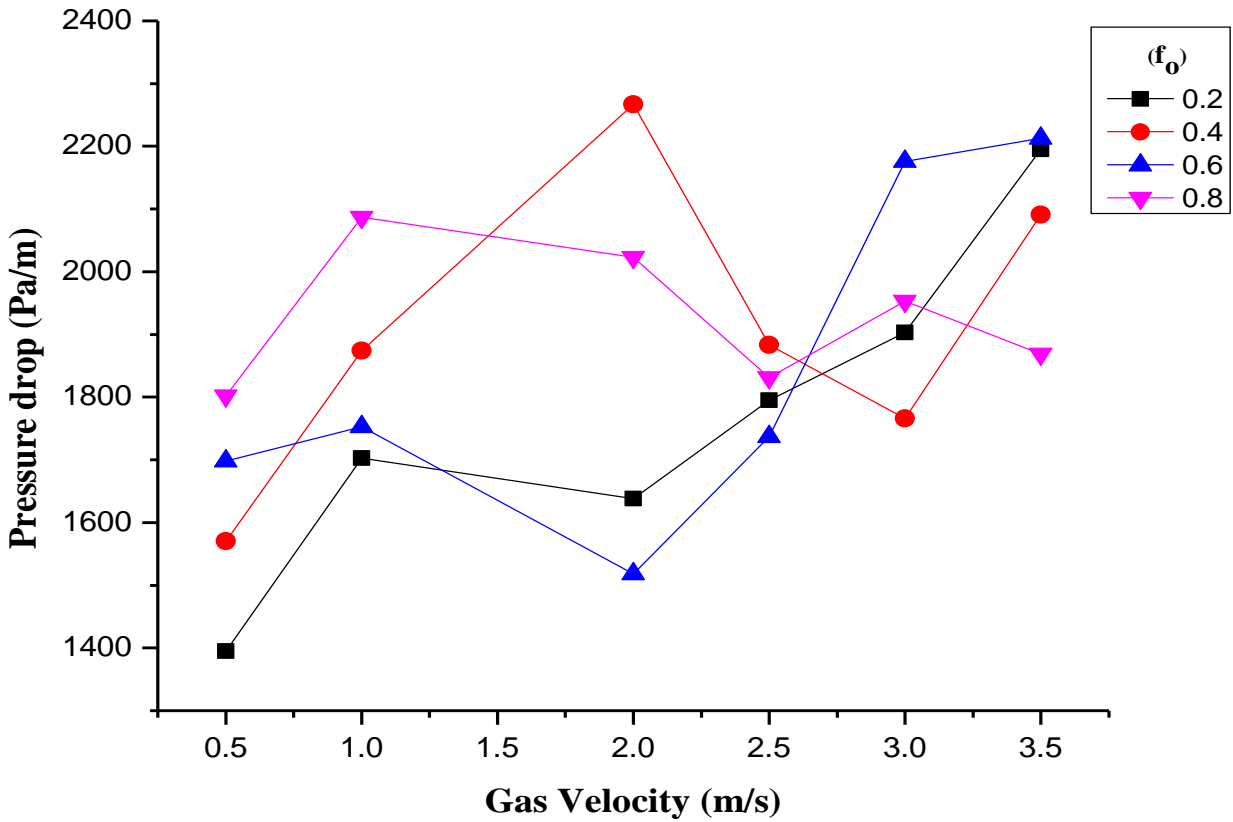


Figure 4.11: Variations in the 180° bend pressure drop at a constant liquid superficial velocity of 0.4 ms⁻¹ with an increasing gas phase superficial velocity and f_0 value.

CHAPTER 5 CONCLUSION AND FUTURE RECOMMENDATIONS

Using the commercial Computational Fluid Dynamics (CFD) software tool ANSYS Fluent, extensive simulation work has been done to examine the fluid pressure drop and gas-oil-liquid three-phase flow patterns in the 90° bend and 180° bend pipes. The CFD tool proved to be very impressive in examining the fluid behaviors and the loss in pressure across the bends. The three-dimensional (3D) geometries of the 90° bend and 180° bend pipes having 6 inches internal diameter and R/d ratio of 1 were constructed to study the effect of individual superficial velocities of the three-phases. The horizontal and vertical lengths of both pipes were 4m and 3m respectively. The gas, oil, and water all had surface velocities between 0.5 and 4 ms⁻¹, 0.08 and 0.36 ms⁻¹, and 0.08 and 0.36 ms⁻¹, respectively. Analysis and comparison with the experimental work have been done for the flow patterns and the pressure drops across the bend.

Three-phase flow patterns identified during 90° bend and 180° bend pipe are Slug, Pseudo-slug, and Rolling Wave flow patterns. All three-phase flow patterns observed in the bend section were to be dependent on the individual phase's superficial velocities. A slug flow pattern was observed during low gas and liquid phase superficial velocities. During the slug flow pattern, the bend section area was fully loaded with the liquid phases and there was less space available for the gas phase to flow through the bend section. The liquid phases might be found to be a distinct layer, a flow that was partially mixed, or a completely mixed flow. Slug flow changed to pseudo-slug flow when the gas phase superficial velocities were raised. The liquid phase flows at the upper outer section of the bend and the gas phase flows at the inner section of the bend. A wave-like structure has been observed during the pseudo-slug flow pattern.

Due to density difference, water being the heaviest phase flows at the bottom of the bend section, oil being lighter than water flows in the middle of the pipelines, and gas which is the lightest one flows at the upper section of the pipe. The pseudo-slug flow is then converted into a rolling wave flow pattern when gas superficial velocities are further increased. The effect of gas velocity produces the rolling wave flow pattern which mainly blows the liquid phase in the bend section at high velocity. Consequently, at greater gas phase velocities, a rolling wave flow pattern was noticed. The liquid phases are present in the bend section as a mixture flow during the rolling wave flow pattern. The

simulation results of three-phase flow patterns observed in the 90° bend and 180° bend were compared with the experimental work. There is good agreement between the three-phase patterns of flow which was observed experimentally.

Pressure drops during 90° bend and 180° bend cross-section pipe has been analyzed thoroughly. Three-phase flow pressure drops were studied in three different scenarios and were compared with the experimental work. A numerical analysis was performed on the pressure drops throughout the 90° bend at a constant f_o value of 0.5 and rising gas and liquid surface velocities. When the simulated and experimental pressure drop findings were compared, there was a good amount of agreement, with an average error of 10.37%.

Furthermore, with two f_o values of 0.25 and 0.75, rising gas superficial velocities, and a constant liquid velocity of 0.32 ms^{-1} were used to mimic the pressure drop across 90° bend. Plotting the pressure drop simulation findings against the experimental pressure drop results revealed a very close match, with an average error of 12.63%.

Additional analysis of the three-phase flow pressure drops was done at increasing gas superficial velocities, constant liquid velocities of 0.4 ms^{-1} , and increasing f_o values from 0.2 to 0.8. Plotting the simulation's pressure drop results against the experimental pressure drop results was done at increasing f_o value. With an average error of 9.03%, the comparison revealed effective communication between the models and strong consensus.

The future recommendations based on the results of current research work are given below:

- The high-viscosity oil can be used in the three-phase flow system. Therefore, the information and analysis obtained through CFD simulations about the fluid flow dynamics which involve the oils with higher viscosity can be very useful.
- During extreme weather conditions, the external temperature would have a significant impact on the viscosity of the phases and pipeline networks. Therefore, the pressure drops during the bends and three-phase flow patterns needed to be studied in extreme weather conditions.
- During the Slug flow, the pressure decreases were mostly oscillating at low gas phase superficial velocities. Consequently, further research is essential to identify the slug flow behavior during the bend flow.

REFERENCES

- [1] Desamala, A.B., A.K. Dasamahapatra, and T.K. Mandal, Oil-water two-phase flow characteristics in horizontal pipeline—a comprehensive CFD study. *International journal of Chemical, Molecular, Nuclear, Materials and Metallurgical Engineering, World Academy of Science, Engineering and Technology*, 2014. **8**(4): p. 360-364.
- [2] Hu, D.-f., et al., Numerical simulation of gas-liquid flow through a 90° duct bend with a gradual contraction pipe. *Journal of Zhejiang University-SCIENCE A*, 2017. **18**(3): p. 212-224.
- [3] Mazumder, Q.H., CFD analysis of the effect of elbow radius on pressure drop in multiphase flow. *Modelling and Simulation in Engineering*, 2012. **2012**: p. 37-37.
- [4] Cazarez, O., et al., Modeling of three-phase heavy oil–water–gas bubbly flow in upward vertical pipes. *International Journal of Multiphase Flow*, 2010. **36**(6): p. 439-448.
- [5] Yaqub, M.W. and R. Pendyala, Experimental investigation of three-phase flow regime transition in a large diameter 90 bend and the resultant pressure drop prediction. *Industrial & Engineering Chemistry Research*, 2022. **61**(20): p. 7090-7102.
- [6] Azzopardi, B.J., et al., Persistence of frequency in gas–liquid flows across a change in pipe diameter or orientation. *International journal of multiphase flow*, 2014. **67**: p. 22-31.
- [7] Kim, S., et al., Geometric effects of 90-degree Elbow in the development of interfacial structures in horizontal bubbly flow. *Nuclear Engineering and Design*, 2007. **237**(20-21): p. 2105-2113.
- [8] Saidj, F., et al., Experimental investigation of air–water two-phase flow through vertical 90 bend. *Experimental thermal and fluid science*, 2014. **57**: p. 226-234.
- [9] Bressani, M. and R.A. Mazza, Two-phase slug flow through an upward vertical to horizontal transition. *Experimental Thermal and Fluid Science*, 2018. **91**: p. 245-255.
- [10] Qiao, S. and S. Kim, Air-water two-phase bubbly flow across 90 vertical elbows. Part I: Experiment. *International Journal of Heat and Mass Transfer*, 2018. **123**: p. 1221-1237.
- [11] Vieira, R.E., et al., Experimental investigation of the effect of 90 standard elbow on horizontal gas–liquid stratified and annular flow characteristics using dual wire-mesh sensors. *Experimental thermal and fluid science*, 2014. **59**: p. 72-87.
- [12] Azzi, A. and L. Friedel, Two-phase upward flow 90 bend pressure loss model. *Forschung im Ingenieurwesen*, 2005. **69**(2): p. 120-130.

- [13] Benbella, S., M. Al-Shannag, and Z.A. Al-Anber, Gas-liquid pressure drop in vertical internally wavy 90 bend. *Experimental Thermal and Fluid Science*, 2009. **33**(2): p. 340-347.
- [14] Bowden, R. and S. Yang, Experimental investigation of two-phase bubbly flow pressure drop across a horizontal pipe containing 90 o bends. *CNL Nuclear Review (Online)*, 2017. **6**(1): p. 55-69.
- [15] Kim, S., et al. Two-phase frictional pressure loss in horizontal bubbly flow with 90-degree bend.
- [16] Yan, X., C.D. Rennie, and A. Mohammadian, A three-dimensional numerical study of flow characteristics in strongly curved channel bends with different side slopes. *Environmental Fluid Mechanics*, 2020. **20**: p. 1491-1510.
- [17] Açıkgöz, M., F. Franca, and R.T. Lahey Jr, An experimental study of three-phase flow regimes. *International Journal of Multiphase Flow*, 1992. **18**(3): p. 327-336.
- [18] Spedding, P.L., G.F. Donnelly, and J.S. Cole, Three phase oil-water-gas horizontal co-current flow: I. Experimental and regime map. *Chemical Engineering Research and Design*, 2005. **83**(4): p. 401-411.
- [19] Lee, A.H., J.Y. Sun, and W.P. Jepson. Study of flow regime transitions of oil water-gas mixtures in horizontal pipelines. *ISOPE*.
- [20] Keskin, C., H.-Q. Zhang, and C. Sarica. Identification and classification of new three-phase gas/oil/water flow patterns. in *SPE Annual Technical Conference and Exhibition? 2007*. SPE.
- [21] Yunus, A.C., *Fluid Mechanics: Fundamentals And Applications (Si Units)*. 2010: Tata McGraw Hill Education Private Limited.
- [22] Lee, A., J. Sun, and W. Jepson. Study of flow regime transitions of oil water-gas mixtures in horizontal pipelines. in *ISOPE International Ocean and Polar Engineering Conference*. 1993. *ISOPE*.
- [23] Açıkgöz, M., F. Franca, and R.J.I.J.o.M.F. Lahey Jr, An experimental study of three-phase flow regimes. 1992. **18**(3): p. 327-336.
- [24] Oddie, G., et al., Experimental study of two and three phase flows in large diameter inclined pipes. 2003. **29**(4): p. 527-558.

- [25] Spedding, P., et al., Three phase oil-water-gas horizontal co-current flow: I. Experimental and regime map. 2005. **83**(4): p. 401-411.
- [26] Bannwart, A.C., et al., Experimental investigation on liquid–liquid–gas flow: Flow patterns and pressure-gradient. 2009. **65**(1-2): p. 1-13.
- [27] Roshani, G., et al., Intelligent recognition of gas-oil-water three-phase flow regime and determination of volume fraction using radial basis function. 2017. **54**: p. 39-45.
- [28] Spedding, P., et al., Pressure drop in three-phase oil–water–gas horizontal co-current flow: experimental data and development of prediction models. 2008. **3**(5): p. 531-543.
- [29] Pietrzak, M., et al., Upward flow of air-oil-water mixture in vertical pipe. 2017. **81**: p. 175-186.
- [30] Bannwart, A.C., et al., Experimental investigation on liquid–liquid–gas flow: Flow patterns and pressure-gradient. *Journal of Petroleum Science and Engineering*, 2009. **65**(1-2): p. 1-13.
- [31] Woods, G., et al., Three-phase oil/water/air vertical flow. 1998. **76**(5): p. 571-584.
- [32] Spedding, P., et al., Flow pattern, holdup and pressure drop in vertical and near vertical two-and three-phase upflow. 2000. **78**(3): p. 404-418.
- [33] Spedding, P.L., E. Bénard, and G.F. Donnelly, Prediction of pressure drop in multiphase horizontal pipe flow. *International communications in heat and mass transfer*, 2006. **33**(9): p. 1053-1062.
- [34] Ayegba, P.O., et al., Applications of artificial neural network (ANN) method for performance prediction of the effect of a vertical 90 bend on an air–silicone oil flow. *Journal of the Taiwan Institute of Chemical Engineers*, 2017. **74**: p. 59-64.
- [35] Mandal, S.N. and S.K. Das, Pressure losses in bends during two-phase gas– Newtonian liquid flow. *Industrial & engineering chemistry research*, 2001. **40**(10): p. 2340-2351.
- [36] Omar, R., B. Azzopardi, and B. Hewakandamby. Air-silicone oil flow around a vertical to horizontal 90 bend. BHR.
- [37] Dong, H., H.Q. Zhang, and C. Sarica. An experimental study of low liquid loading gas-oil-water flow in horizontal pipes. BHR.
- [38] Spedding, P.L., G.F. Donnelly, and E. Benard, Three-phase oil–water–gas horizontal co-current flow part II. Holdup measurement and prediction. *Asia-Pacific Journal of Chemical Engineering*, 2007. **2**(2): p. 130-136.

- [39] Autee, A. and S.J.P.i.S. Giri, Experimental study on two-phase flow pressure drop in small diameter bends. 2016. **8**: p. 621-625.
- [40] Omar, R., B. Azzopardi, and B. Hewakandamby. Air-silicone oil flow around a vertical to horizontal 90 bend. in BHR International Conference on Multiphase Production Technology. 2015. BHR.
- [41] Qiao, S. and S. Kim, On the prediction of two-phase pressure drop across 90 vertical elbows. *International Journal of Multiphase Flow*, 2018. **109**: p. 242-258.
- [42] Sánchez Silva, F., et al., Pressure drop models evaluation for two-phase flow in 90 degree horizontal elbows. *Ingeniería mecánica, tecnología y desarrollo*, 2010. **3**(4): p. 115-122.
- [43] Sobocinski, D.P. and R.L. Huntington, Concurrent Flow of Air, Gas-Oil, and Water in a Horizontal Pipe. *Transactions of the American Society of Mechanical Engineers*, 1958. **80**(1): p. 252-255.
- [44] Shakirov, R.S., Pressure of hydraulic resistances during the motion of gas-oil-water mixtures in pipes. *Gazovoc Delo*, 1969. **11**: p. 17-20.
- [45] Kumar, P. and J. Singh, Computational study on effect of Mahua natural surfactant on the flow properties of heavy crude oil in a 90 bend. *Materials Today: Proceedings*, 2021. **43**: p. 682-688.
- [46] Singh, J., et al., CFD modeling of erosion wear in pipe bend for the flow of bottom ash suspension. *Particulate Science and Technology*, 2019. **37**(3): p. 275-285.
- [47] Yaqub, M.W., et al., Review on gas-liquid-liquid three-phase flow patterns, pressure drop, and liquid holdup in pipelines. *Chemical Engineering Research and Design*, 2020. **159**: p. 505-528.
- [48] Zhang, H.-Q. and C. Sarica, Unified modeling of gas/Oil/Water-Pipe flow-basic approaches and preliminary validation. *SPE Projects, Facilities & Construction*, 2006. **1**(02): p. 1-7.
- [49] Yaqub, M.W., R. Rusli, and R. Pendyala, Experimental study on gas-liquid-liquid three-phase flow patterns and the resultant pressure drop in a horizontal pipe upstream of the 90° bend. *Chemical Engineering Science*, 2020. **226**: p. 115848.
- [50] Kühnen, J., et al., Experimental investigation of transitional flow in a toroidal pipe. *Journal of fluid mechanics*, 2014. **738**: p. 463-491.

- [51] Pantokratoras, A., Steady laminar flow in a 90 bend. *Advances in Mechanical Engineering*, 2016. **8**(9): p. 1687814016669472.
- [52] Lupi, V., J. Canton, and P. Schlatter. On the onset of transition in 90°-bend pipe flow. *International Symposium on Turbulence and Shear Flow Phenomena, TSFP*.
- [53] Paolinelli, L.D. Study of Phase Wetting in Three-Phase Oil-Water-Gas Horizontal Pipe Flow—Recommendations for Corrosion Risk Assessment. *NACE*.
- [54] Wang, H.Q., Y. Wang, and L. Zhang, Characteristics of pressure gradient fluctuation for oil-gas-water three-phase flow based on flow pattern. *Applied Mechanics and Materials*, 2011. **66**: p. 1187-1192.
- [55] Shmueli, A., T.E. Unander, and O.J. Nydal. Characteristics of gas/water/viscous oil in stratified-annular horizontal pipe flows. *OTC*.
- [56] Qiang, W., et al., Experimental tomographic methods for analysing flow dynamics of gas-oil-water flows in horizontal pipeline. *Journal of Hydrodynamics, Ser. B*, 2016. **28**(6): p. 1018-1021.
- [57] Ribeiro, J.X.F., et al., Experimental study of horizontal two-and three-phase flow characteristics at low to medium liquid loading conditions. *Heat and Mass Transfer*, 2019. **55**: p. 2809-2830.
- [58] Pietrzak, M., M. Płaczek, and S. Witczak, Upward flow of air-oil-water mixture in vertical pipe. *Experimental Thermal and Fluid Science*, 2017. **81**: p. 175-186.
- [59] Shmueli, A., T. Unander, and O. Nydal. Characteristics of gas/water/viscous oil in stratified-annular horizontal pipe flows. in *Offshore Technology Conference Brasil*. 2015. *OTC*.
- [60] Wang, H.Q., et al., Characteristics of pressure gradient fluctuation for oil-gas-water three-phase flow based on flow pattern. 2011. **66**: p. 1187-1192.
- [61] Wu, H., F. Zhou, and Y.J.I.J.o.M.F. Wu, Intelligent identification system of flow regime of oil–gas–water multiphase flow. 2001. **27**(3): p. 459-475.
- [62] Wegmann, A., J. Melke, and P.R.J.I.J.o.M.F. von Rohr, Three phase liquid–liquid–gas flows in 5.6 mm and 7 mm inner diameter pipes. 2007. **33**(5): p. 484-497.
- [63] Hu, B., et al., Development of an X-ray computed tomography (CT) system with sparse sources: application to three-phase pipe flow visualization. 2005. **39**: p. 667-678.

- [64] Liu, X.-m., et al., Experimental study of flow patterns and pressure drops of heavy oil-water-gas vertical flow. *Journal of Hydrodynamics, Ser. B*, 2014. **26**(4): p. 646-653.
- [65] Xie, B., et al., Analysis of vertical upward oil-gas-water three-phase flow based on multi-scale time irreversibility. 2018. **62**: p. 9-18.
- [66] Gao, Z.-K., et al., Visibility graphs from experimental three-phase flow for characterizing dynamic flow behavior. 2012. **23**(10): p. 1250069.
- [67] Gao, Z.-K. and N.-D.J.C.E.S. Jin, Nonlinear characterization of oil-gas-water three-phase flow in complex networks. 2011. **66**(12): p. 2660-2671.
- [68] Wang, D.-Y., et al., Measurement of gas phase characteristics in vertical oil-gas-water slug and churn flows. *Chemical Engineering Science*, 2018. **177**: p. 53-73.
- [69] Wang, D.-Y., et al., Development of a rotating electric field conductance sensor for measurement of water holdup in vertical oil-gas-water flows. *Measurement Science and Technology*, 2018. **29**(7): p. 075301.
- [70] Wang, D.-Y., et al., Development of a rotating electric field conductance sensor for measurement of water holdup in vertical oil-gas-water flows. 2018. **29**(7): p. 075301.
- [71] Oddie, G., et al., Experimental study of two and three phase flows in large diameter inclined pipes. *International journal of multiphase flow*, 2003. **29**(4): p. 527-558.
- [72] Rodriguez, O.M.H. and R.V.A. Oliemans, Experimental study on oil-water flow in horizontal and slightly inclined pipes. *International Journal of Multiphase Flow*, 2006. **32**(3): p. 323-343.
- [73] Jana, A.K., G. Das, and P.K. Das, Flow regime identification of two-phase liquid-liquid upflow through vertical pipe. *Chemical engineering science*, 2006. **61**(5): p. 1500-1515.
- [74] Ghajar, A.J. and C.C. Tang, Heat transfer measurements, flow pattern maps, and flow visualization for non-boiling two-phase flow in horizontal and slightly inclined pipe. *Heat Transfer Engineering*, 2007. **28**(6): p. 525-540.
- [75] Sotgia, G., P. Tartarini, and E. Stalio, Experimental analysis of flow regimes and pressure drop reduction in oil-water mixtures. *International journal of multiphase flow*, 2008. **34**(12): p. 1161-1174.
- [76] Xu, J.-y., et al., Investigations of phase inversion and frictional pressure gradients in upward and downward oil-water flow in vertical pipes. *International Journal of Multiphase Flow*, 2010. **36**(11-12): p. 930-939.

- [77] Zong, Y.-B., et al., Nonlinear dynamic analysis of large diameter inclined oil–water two phase flow pattern. *International Journal of Multiphase Flow*, 2010. **36**(3): p. 166-183.
- [78] Du, M., et al., Flow pattern and water holdup measurements of vertical upward oil–water two-phase flow in small diameter pipes. *International Journal of Multiphase Flow*, 2012. **41**: p. 91-105.
- [79] Al-Wahaibi, T., et al., Experimental investigation on flow patterns and pressure gradient through two pipe diameters in horizontal oil–water flows. *Journal of Petroleum Science and Engineering*, 2014. **122**: p. 266-273.
- [80] Hojati, S.A. and P. Hanafizadeh. Effect of inclination pipe angle on oil-water two phase flow patterns and pressure loss. *American Society of Mechanical Engineers*.
- [81] Sudo, K., M. Sumida, and H. Hibara, Experimental investigation on turbulent flow in a square-sectioned 90-degree bend. *Experiments in Fluids*, 2001. **30**(3): p. 246-252.
- [82] Kim, J., M. Yadav, and S. Kim, Characteristics of secondary flow induced by 90-degree elbow in turbulent pipe flow. *Engineering Applications of Computational Fluid Mechanics*, 2014. **8**(2): p. 229-239.
- [83] Dutta, P., et al., Numerical study on flow separation in 90° pipe bend under high Reynolds number by k- ϵ modelling. *Engineering Science and Technology, an International Journal*, 2016. **19**(2): p. 904-910.
- [84] Abdulkadir, M., et al., Interrogating the effect of 90 bends on air–silicone oil flows using advanced instrumentation. *Chemical Engineering Science*, 2011. **66**(11): p. 2453-2467.
- [85] Musa, V.A., L.A. Abdulkareem, and O.M. Ali, Experimental Study of the Two-Phase Flow Patterns of Air-Water Mixture at Vertical Bend Inlet and Outlet. *Engineering, Technology & Applied Science Research*, 2019. **9**(5): p. 4649-4653.
- [86] Zahedi, R. and A.B. Rad, Numerical and experimental simulation of gas-liquid two-phase flow in 90-degree elbow. *Alexandria Engineering Journal*, 2022. **61**(3): p. 2536-2550.
- [87] Hossain, M., et al., Investigation of slug-churn flow induced transient excitation forces at pipe bend. *Journal of Fluids and Structures*, 2019. **91**: p. 102733.
- [88] Spedding, P.L., E. Bénard, and N.M. Crawford, Fluid flow through a vertical to horizontal 90° elbow bend III three phase flow. *Experimental thermal and fluid science*, 2008. **32**(3): p. 827-843.

- [89] Yaqub, M.W., R. Pendyala, and R. Rusli, Oil-Water Phase Inversion in the Horizontal Section of Upstream 90° Bend during Gas-Oil-Water Three-Phase Flow. *Key Engineering Materials*, 2019. **796**: p. 137-144.
- [90] Yaqub, M.W. and R. Pendyala. CFD simulations of gas-liquid-liquid three-phase co-current flow in horizontal pipe by tracking volume fractions using VOF model. IOP Publishing.
- [91] Lockhart, W.R., Proposed correlation of data for isothermal two-phase, two-component flow in pipes. *Chemical engineering progress*, 1949. **45**(1): p. 39-48.
- [92] Brauner, N., Two-phase liquid-liquid annular flow. *International journal of multiphase flow*, 1991. **17**(1): p. 59-76.
- [93] Poesio, P., D. Strazza, and G. Sotgia, Very-viscous-oil/water/air flow through horizontal pipes: Pressure drop measurement and prediction. *Chemical Engineering Science*, 2009. **64**(6): p. 1136-1142.
- [94] Dehkordi, P.B., et al., A mechanistic model to predict pressure drop and holdup pertinent to horizontal gas-liquid-liquid intermittent flow. *Chemical Engineering Research and Design*, 2019. **149**: p. 182-194.
- [95] Chisholm, V.D., Two-phase flow in bends. *International Journal of Multiphase Flow*, 1980. **6**(4): p. 363-367.
- [96] Sookprasong, P., Two-phase flow in piping components. 1980: University of Tulsa, Fluid Flow Projects.
- [97] Bergman, T.L., *Fundamentals of heat and mass transfer*. 2011: John Wiley & Sons.
- [98] Fluent, A., *ANSYS fluent theory guide 15.0*. ANSYS, Canonsburg, PA, 2013. **33**.